AD-416 53

DASA-1398
URS 170-15

STUDY OF CHANNELING OF AIR BLAST WAVES

Final Report

Prepared for

DEFENSE ATOMIC SUPPORT AGENCY
Washington 25, D.C.

UNITED
RESEARCH

(Woodview Research Corp)

UNITED RESEARCH

CAMBRIDGE, MASSACHUSETTS   NEW YORK, NEW YORK
BURLINGAME, CALIFORNIA   SIERRA VISTA, ARIZONA
BEVERLY HILLS, CALIFORNIA   WASHINGTON, D. C.
CINCINNATI, OHIO

URS 170-15   DASA-1398

STUDY OF CHANNELING OF AIR BLAST WAVES

Final Report

June 26, 1963

by

C. Wilton   N. R. Wallace   K. Kaplan
UNITED RESEARCH SERVICES
Formerly Broadview Research Corporation
1811 Trousdale Drive
Burlingame, California

Prepared for

DEFENSE ATOMIC SUPPORT AGENCY
Washington 25, D.C.
Contract Number DA 49-146-XZ-050

TABLE OF CONTENTS

LIST OF FIGURES

Table of Contents (Cont'd)

List of Figures (Cont'd)

Table of Contents (Cont'd)

List of Figures (Cont'd)

Table of Contents (Cont'd)

List of Figures (Cont'd)

LIST OF TABLES

Section I

INTRODUCTION

During a URS study of the effects of topography on shock waves in air, it was noticed that shock wave over-pressures measured in certain valley configurations from charges exploded over the valleys themselves were higher than would be expected if the effects of the valley sides were considered separately.[1] It appeared evident that the shock wave reflections from the valley sides were inter-acting with each other causing increases in overpressure in certain parts of the valley. If significant, this effect, termed "channeling", could be of importance in the develop-ment of doctrine for the employment of nuclear weapons, especially of tactical weapons.

Under contract DA 49-146-XZ-050 for the Defense Atomic Support Agency (DASA), URS has been conducting a study to determine what charge and topography conditions, if any, result in significant air blast channeling and to determine the magnitude of these effects in certain valley shapes.

The work was largely experimental in nature, and con-sisted of tests in which small-scale valley models were exposed to shock waves from small high-explosive charges. Shock wave parameters were measured on the slopes and at the bottom of the valleys. Preliminary theoretical work was done to aid in the design of the test program and of the models.

In Section II of this report, the theoretical work is described, and in Section III the design and conduct of the experimental program is discussed. In Section IV, the results of the program are summarized, and in Section V, conclusions and recommendations derived from results of the program are presented.

The principal investigators on the study were Mr. C. Wilton, who was in charge of the experimental program, and

---

[1] See Reference 1.

Mr. N. R. Wallace, who conducted the theoretical investigation. Messrs. A. B. Willoughby and K. Kaplan participated in program planning and data analysis, and Mr. J. Boyes in the field portions of the test program.

The cooperation of Lt. Col. C. C. Clifford, DASA Project Officer, and Lt. Col. D. Baker, Office of Chief of Research and Development, Department of Army, is gratefully acknowledged.

Section II

THEORETICAL CONSIDERATIONS

Preliminary estimates were made of the magnitude and location of significant channeling effects for one of the valley configurations considered for study. The results of this work formed a basis for design of the experimental test program and the scale models. The valley considered was two-dimensional in the usual sense of being uniform in cross section. The calculations were for the symmetrical case of a charge located in the plane bisecting the plane surfaces that form the valley. All calculations were for the particular case of a 110-gram charge.

It follows immediately from consideration of image charge effects that for ideally rigid surfaces, a charge fired at the surface on the bottom of a V-shaped valley scales to an equivalent free-air burst according to the angle included by the valley walls. A charge fired on a flat, rigid surface has an effective weight of twice the charge weight (2W), and a charge fired in a 90-degree corner has an effective weight of four times the actual weight (4W). The case treated was that of a 30-degree symmetrical valley. The angle included between the sides is 120 degrees, giving a charge fired at the valley bottom the effective weight of 3W.

Only one shock develops, the initial shock from the burst. It expands outwards from the charge without any reflections at the valley bottom. This must be so since the shock front is normal to each of the valley slopes and is consequently normal to any line drawn through the inter-section of the valley slopes.

When the shock front first reaches the edge of a finite valley slope, a rarefaction starts back down the slope to eventually decrease the strength of the expanding shock in the valley proper. If the topography exterior to the valley is a flat plain, the shock front traveling along the valley bottom and decaying initially according to the fall-off curve for a charge weight of 3W will at large distances decay

according to the fall-off curve for an effective charge weight of 2W. Given the fall-off curve of overpressure versus scaled distance (ft/W$^{1/3}$), the maximum amplicication factor in the valley relative to the flat plain is obtained from the ratio of the overpressure at a given distance for a charge weight of 3W to the overpressure at the same distance for a charge weight of 2W.

Although important as a limiting case, a surface burst in the bottom of a valley does not possess the tactical interest of an elevated burst. For the symmetrical case remarked previously, accurate predictions of peak overpressure at the intersection of the valley slopes can be made so long as the shock reflection remains regular.

Figure 1.a is a sketch of the shocks reflected from the valley slopes and their interaction; the incident spherical shock is not shown. Figures 1.b, 1.c, and 1.d show three stages of the reflection (in cross section) from the valley bottom directly below the burst.

The plane bisecting the valley slopes contains the charge and represents a surface across which no particle flow occurs in the reflection process. If the height of burst (HOB) is measured from the charge along the normal to the valley bottom, the strength of the incident shock at the bottom is given by the charge weight and distance from a pressure versus reduced distance curve. Provided the point of calculation is essentially at the line of intersection of the slopes, complete information about the reflected shock (Region 2) is known from the plane shock theory:[1]

$$-M^2(1-\mu^2)^2(t_o-t_2)+M\{(1-\mu^2)^2-(t_o-\tau_2)^2$$
$$-(\mu^2+t_o t_2)^2\}-(t_o-t_2)=0$$

---

[1] See Reference 2.
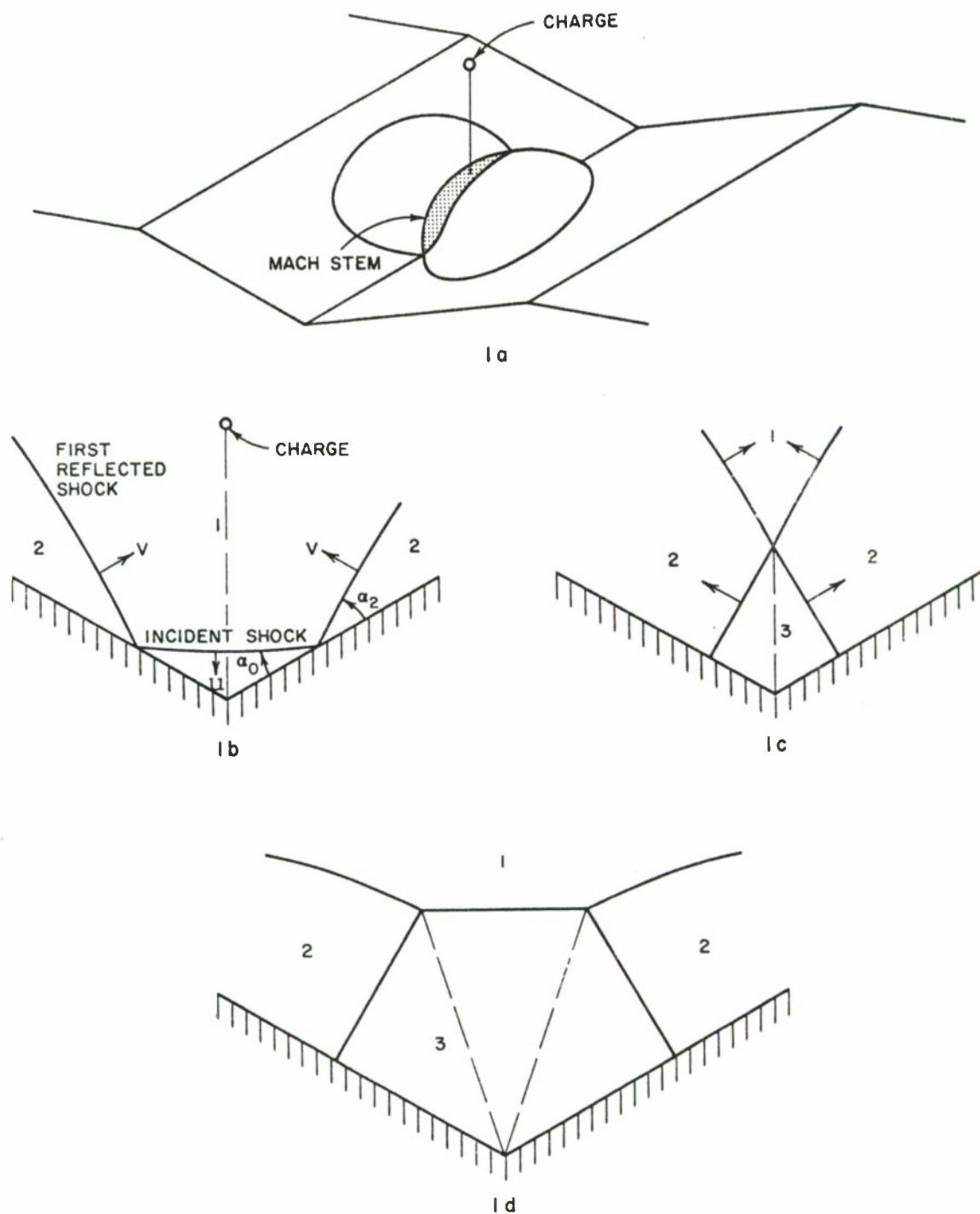
Figure 1

SHOCKS REFLECTED FROM VALLEY SLOPES AND BOTTOM AND THEIR
INTERACTION

where:

$$M = \frac{(1 - \zeta) t^o}{1 + \mu^2 \zeta + (\zeta + \mu^2) t_o^2}$$

$$\zeta = \frac{P_o}{P_1}$$

$$\mu^2 = \frac{\gamma - 1}{\gamma + 1}$$

$$t_o = \tan \lambda_o$$

$$t_2 = \tan \lambda_2$$

M is calculated from Equation 2 with a_o = 30 degrees, and a_2 is determined from Equation 1.

If U and V are the shock velocities of the incident and first reflected shocks with respect to the valley slopes as shown in Figure 1.b, they are related by:

$$\frac{V}{\sin \alpha_2} = \frac{U}{\sin \alpha_o}$$

The particle velocity at the incident shock from q_1 is related to the particle velocity q_2 parallel to the surface behind the first reflected shock by:

$$q_2 \cos \alpha_2 = q_1 \sin (\alpha_o + \alpha_2)$$

The pressure ratio ς across the first reflected shock is obtained from:

$$\frac{(1 - \zeta)^2}{(\mu^2 + \zeta)(1 + t_o^2)} = \frac{(\zeta - 1)^2}{(\mu^2 + \zeta)(1 + t_2^2)}$$

where $\varsigma = P_2/P_1$.

With the shock strength z defined as:

$$z = \frac{P_1 - P_0}{P_0} = \frac{1}{\xi} - 1$$

$$\frac{c_2}{c_0} = \frac{c_2}{c_1} \frac{c_1}{c_0} = \sqrt{\frac{(z+1)(z+7)\xi(6+\xi)}{(7+6z)(1+6\xi)}}$$

where c is the velocity of sound, and γ is taken as 7/5.

The strength of the reflected shock separating Region 3 from Region 2 is that required to bring the flow in Region 2 to rest. Thus, if $\Omega = (P_3 - P_2)/P_2$, then in order that $q_3 = -q_2$:

$$\frac{q_3}{c_2} = \frac{6\Omega + 7}{7} \cdot \frac{5\Omega}{7 + 6\Omega} = \frac{-q_2}{c_2}$$

or

$$25\Omega^2 - 42 \frac{q_2^2}{c_2^2} \Omega - 49 \frac{q_2^2}{c_2^2} = 0$$

The peak pressure P at ground zero in the valley bottom is given by:

$$\frac{P}{P_0} = \frac{1}{\xi} \cdot \zeta \cdot (\Omega + 1)$$

and is plotted in Figure 2 versus shock strength.

Figure 3 is a scaled drawing of the left portion of the situation shown in Figure 1.c for three incident shock strengths ξ. Note that for the 30-degree valley discussed here, the reflection from the bottom is regular. Instead of basing the calculation of overpressure in Region 3 on the requirement that the flow in Region 2 be stopped, the same techniques used to determine thermodynamic properties in Region 2 could have been used. The method followed is not only easier but also has the advantage of giving the shock
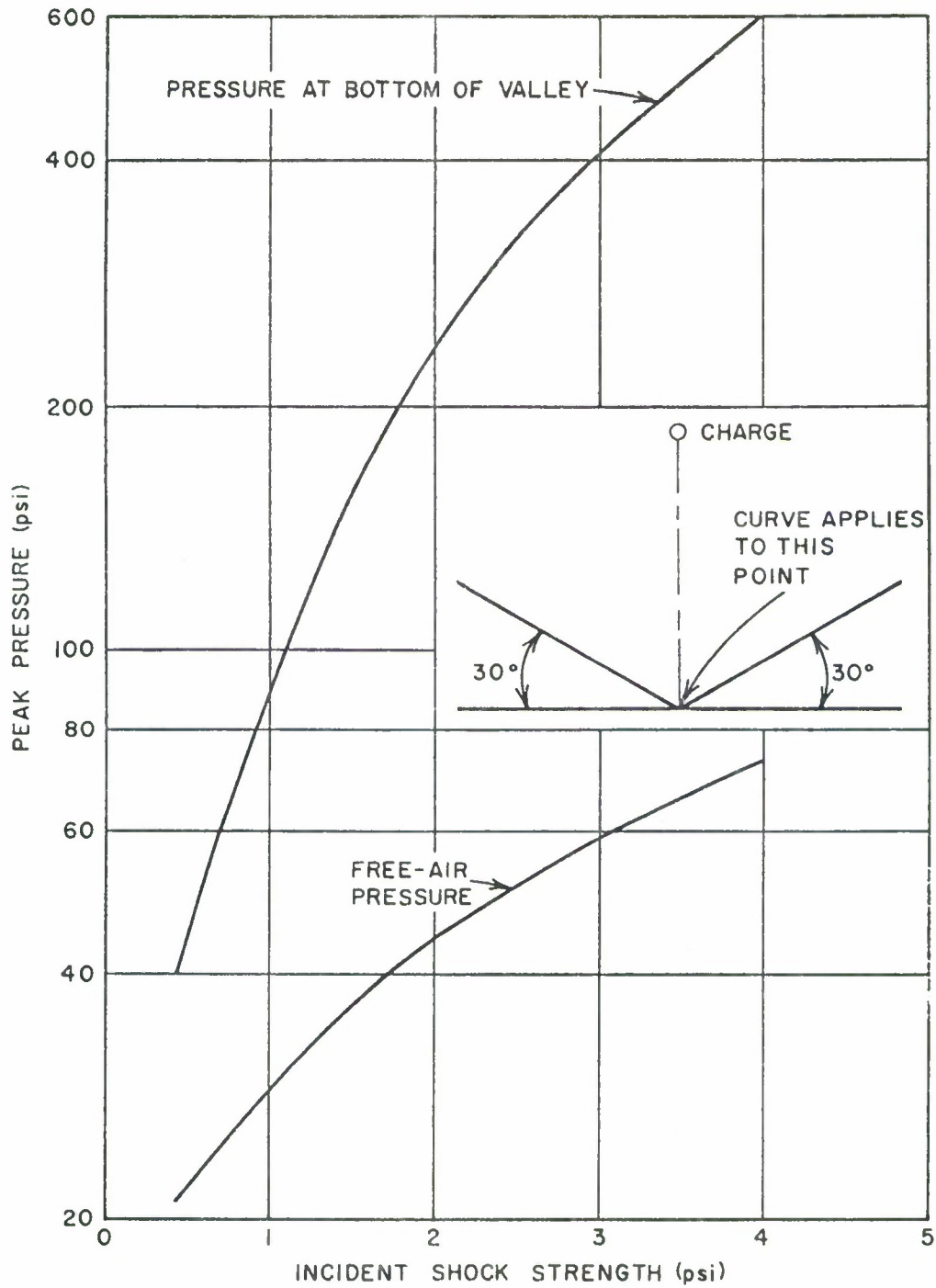
Figure 2

PEAK PRESSURE ON THE BOTTOM OF A 30-DEGREE VALLEY AT GROUND
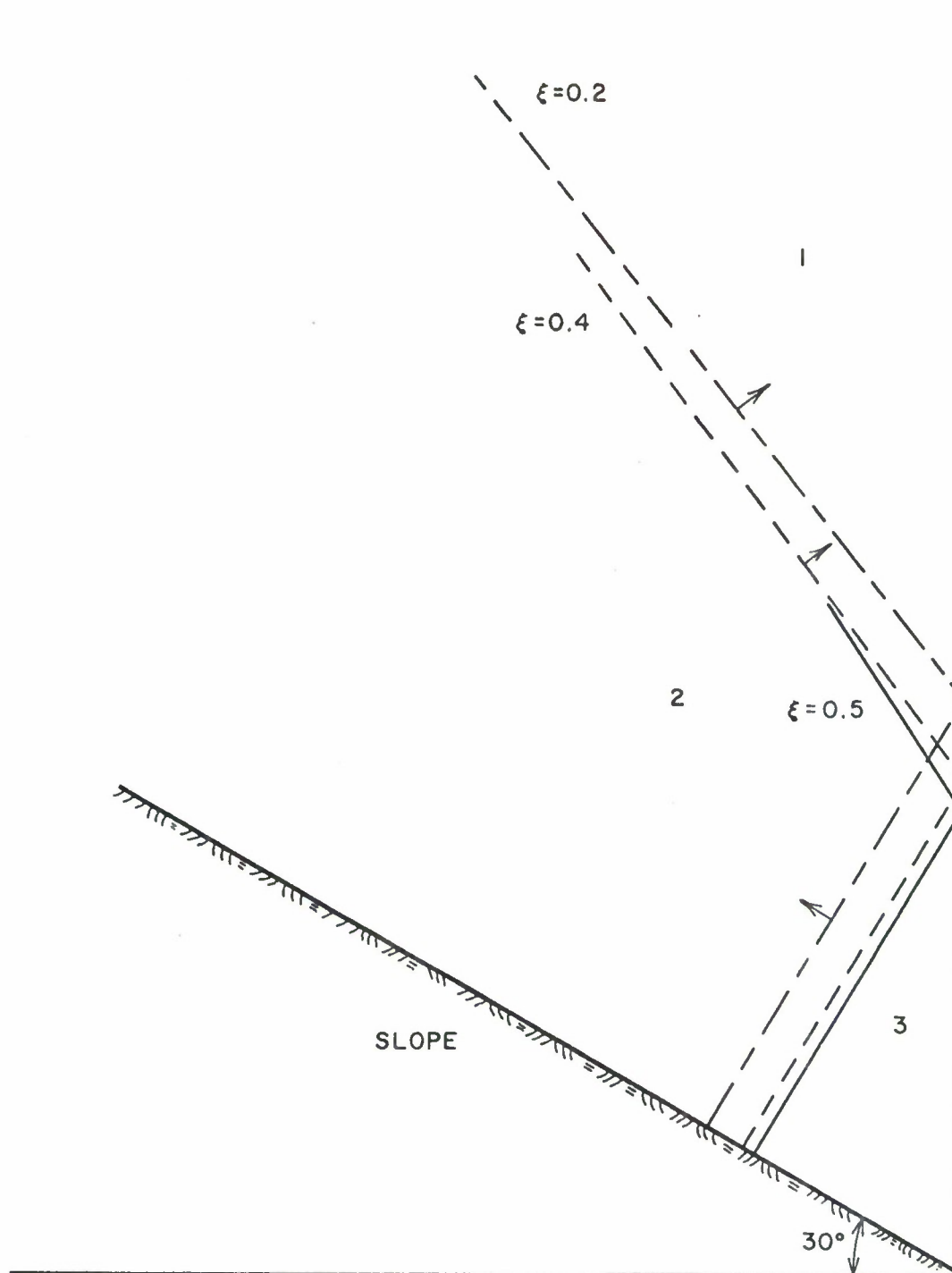ZERO COMPARED WITH PEAK PRESSURE FOR A FREE-AIR SHOCK

Figure 3

CROSS SECTION OF REFLECTION FROM VALLEY BOTTOM FOR THREE
DIFFERENT SHOCK STRENGTHS

configuration even if the first reflected shock shares a
Mach stem with its image (See Figure 1.d.) as is the case
for a 15-degree symmetrical valley. This Mach stem inevi-
tably forms as the first reflected shocks proceed upwards
from the bottom of the valley even if it is not present
when the incident shock first reflects from the valley
bottom (as shown in Figure 1.a).

As the point of contact of the incident spherical shock
moves along the line of intersection of the valley slopes,
regular reflection gives way to Mach reflection. If can
easily be shown that Mach reflection develops first at the
slope intersection line before it occurs anywhere else on
the valley slopes. Thereafter, simple calculations can no
longer yield reliable values of peak overpressure. At any
distance between this transition point and ground zero, peak
overpressure can be calculated by the method described except
that the velocity component at the surface normal to the line
of slope intersection must be stopped by the shock reflected
from the bisecting plane. It should be observed that the
shock that generates Region 3, which has been referred to as
the shock "reflected from the bisecting plane" or as the
shock that "halts the particle flow," is in fact that part
of the first reflected shock that is transmitted through the
bisecting plane from the other slope.

Ground zero peak pressure was calculated for each of
five incident shock strengths, viz. 0.2, 0.4, 0.5, 0.6, and
0.7. An additional point was calculated for each shock
strength at the position where the regular to Mach reflec-
tion transition occurs along the valley bottom. In Figure
4, HOB curves for the bottom of a 30-degree symmetrical
valley have been sketched through the calculated points,
using HOB curves for the flat plain (2W) situation and
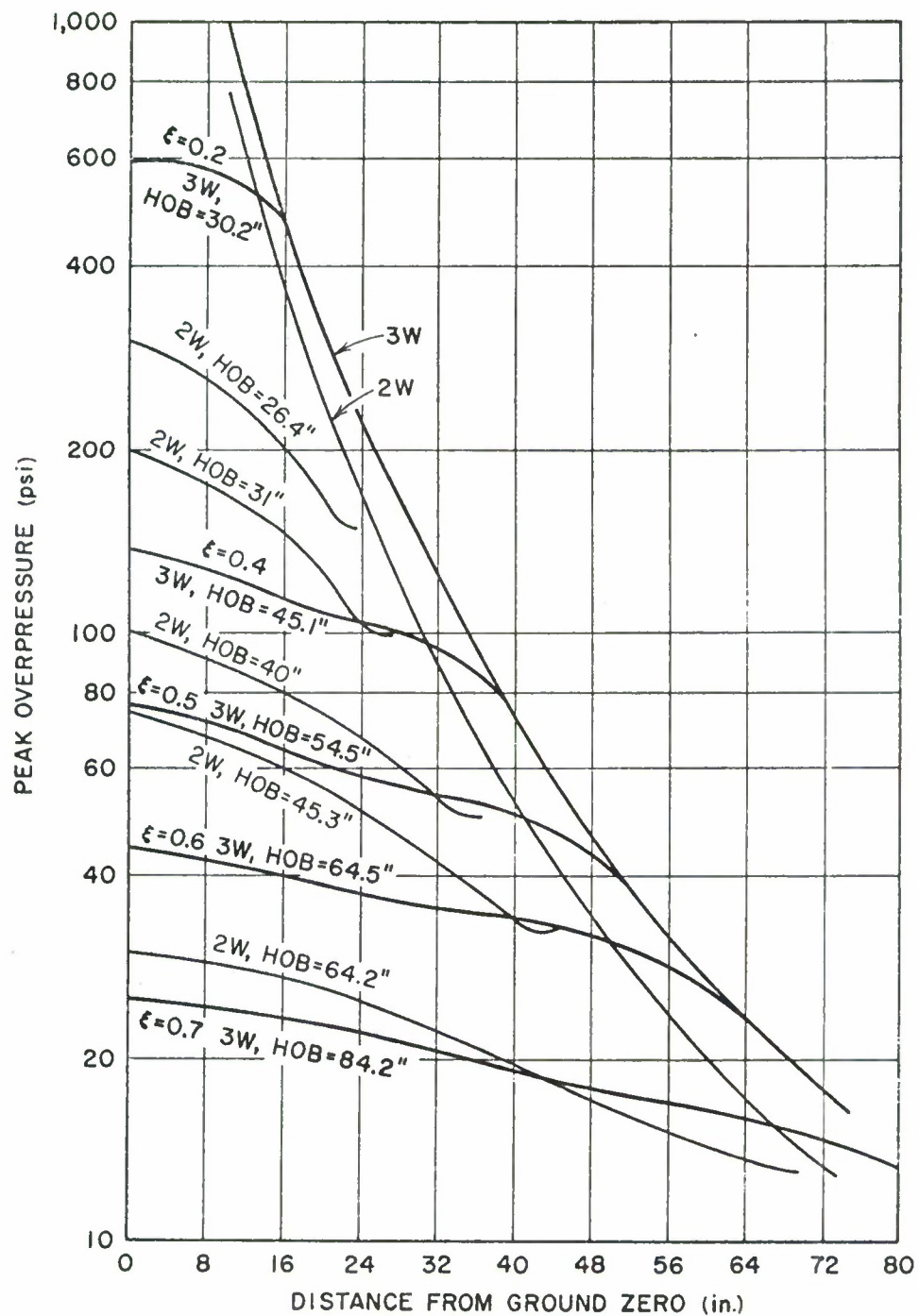fall-off curves for 2W and 3W as guides.

Figure 4

HEIGHT OF BURST (HOB) CURVES (3W) FOR A 110-GRAM CHARGE
FIRED AT THE BOTTOM OF A 30-DEGREE VALLEY

Section III

DESIGN OF THE EXPERIMENTAL TEST PROGRAM

The principle objectives of the experimental test program were to determine the conditions under which significant channeling of air blast can occur and to determine the magnitude of these effects. The technique used was to subject generalized valley shapes to air blast from small high-explosive charges and to measure the air blast parameters within the valleys.

Only a relatively small number of the variations in valley and explosive charge characteristics that could conceivably influence the occurrence and magnitude of the channeling effect could be considered. All valleys examined had straight sides, were two-dimensional (that is uniform in cross section along the valley axis), and were bordered by flat terrain. Both V-bottomed and flat-bottomed valleys, representative of commonly occurring natural valleys, were examined. Other valley characteristics that were varied were the slope angles of the valley sides (relative to each other and to flat terrain) and the lengths of the valley sides normal to its axis.

Explosive charges were placed directly over the valley axis and over the valley sides at various elevations above the valley floor. Initially the size of the explosive charge was also to be varied, but instead, the effect of charge size variation was obtained by changing the length of the valley sides. The importance of charge size is important primarily in deforming the length of the generated shock wave relative to the size of the valley.

Throughout this program, full-scale criteria used as a basis for scaling were weapon sizes of 20 to 200 kilotons, and valley slope lengths of around 1,000 feet. The presure range of interest was assumed to be from 100 to 7 psi.

TEST PLAN

A total of 36 tests were planned and conducted in six generalized valley shapes, viz., three sizes of 30-degree V-bottom valleys, two widths of 30-degree flat-bottom valleys, and a 15-degree V-bottom valley.

The valley models used were 12 feet long with basic slope lengths normal to the valley axis of 27 inches. (Nine and eighteen inch slope lengths were also used.) From the top edges of the slopes, flat planes were extended for sufficient distances on either side of the valley to keep spurious signals from the edges of the planes from reaching the gauge stations in the valley during the time of interest. Figure 5 shows all model layouts except the 15-degree V-bottom valley and the flat-terrain model. Gauge lines extend along one slope only at 18, 36, 60, 84, and 108 inches from ground zero (GZ). From two to six gauge positions were used on each gauge line depending on the particular valley model being tested.

Five charge positions were used, viz., 7, 30, and 51 inches over the center of the valley and 30 and 51 inches, measured from the bottom of the valley, over the left and right top edges of the 30-degree V-bottom valley. Table I summarizes the test plan for the entire program.

For the 110-gram RDX charges used, the basic 27-inch slope length of the model scales to 970 feet for a 20-kiloton weapon and 2,090 feet for a 200-kiloton weapon. The incident overpressures of interest, 100 to 7 psi, occur at horizontal distances of 18 to 108 inches from GZ for a 30-inch HOB.

The first three test situations in which 30-degree V-bottomed valleys with slope lengths of 9, 18, and 27 inches were used in succession had a twofold purpose:

1. To simulate a change in charge size, since changing the slope length for a fixed weight of charge can be considered the same in a scaled sense as changing the charge weight for a fixed slope length. Thus, tests on a model with 9-, 18-, and 27-inch slopes,

PLAN VIEW OF
CHARGE LOCATIONS

51 in.

30 in.

7 in.

30°   30°

R

L

V-BOTTOM 30-degree VALLEY

GZ = 0

18 in.
36 in.
60 in.
84 in.
108 in.
INCHES FROM GROUND ZERO

12 FT

30°

30°

R

L

VALLEY BOTTOM OF TWO THIRDS
THE SLOPE LENGTH

18 in.

30°

30°

VALLEY BOTTOM OF ONE THIRD
THE SLOPE LENGTH

9 in.

27 in.

30°

30°
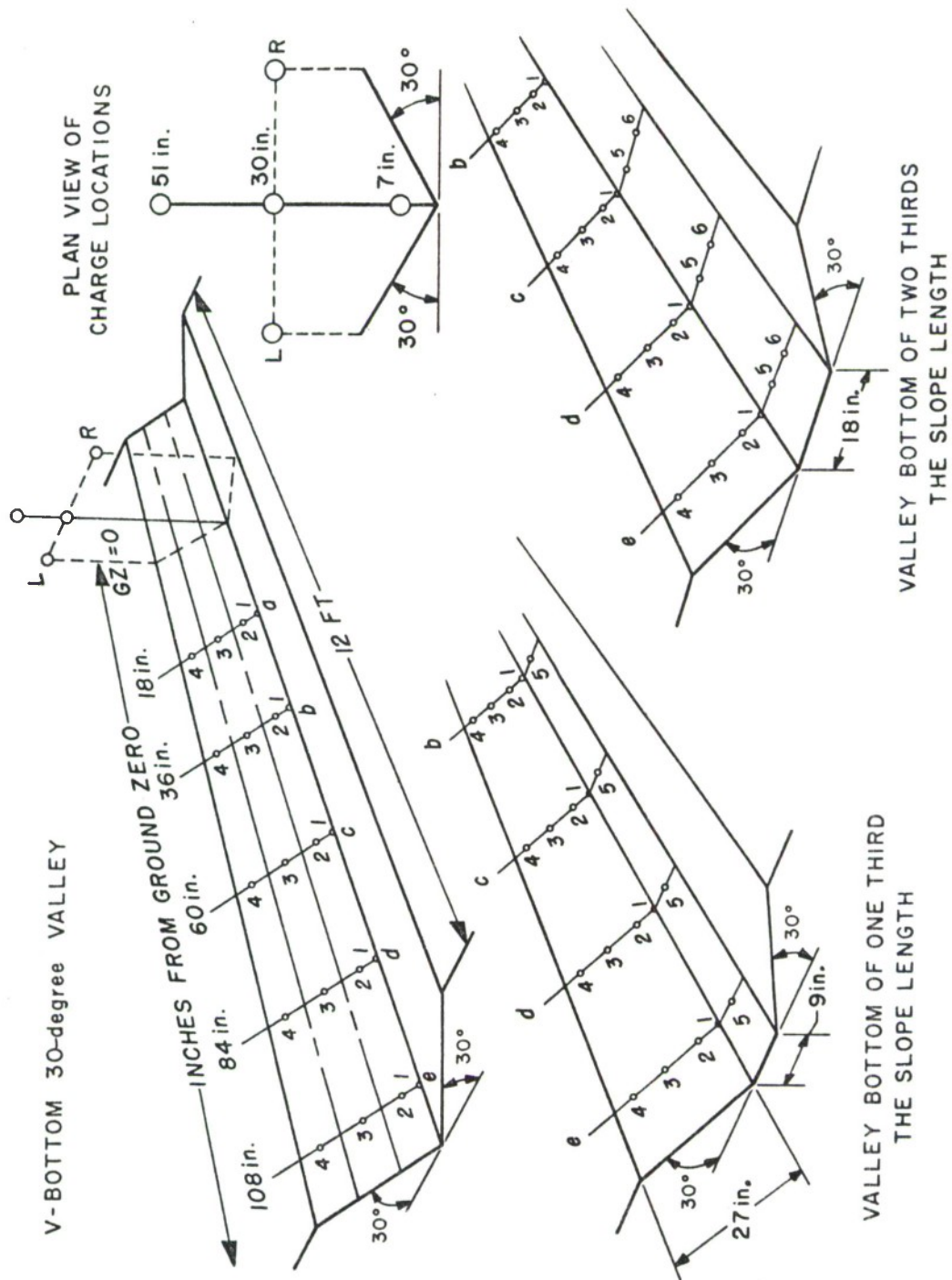
Figure 5

MODEL DESIGN

Table I

TEST PLAN

			Description			
Test Situation	Number of Shots	Charge Position	Height of Burst (inches)	Slope Length (inches)	Valley Bottom (inches)	Single Slope Angle
A	2	Center	30	9	0	30°
B	3	Center	30	18	0	30
C	3	Center	30	27	0	30
D	3	Center	51	27	0	30
E	3	Left	51	27	0	30
F	3	Right	51	27	0	30
G	3	Right	30	27	0	30
H	3	Left	30	27	0	30
I	3	Center	7	27	0	30
J	3	Center	30	27	9	30
K	4	Center	30	27	18	30
L	3	Center	30	27	0	15
M	3	Center	7	Flat Terrain		
N	3	Center	30	Flat Terrain		
O	3	Center	51	Flat Terrain		

all with the same charge weight are equivalent to tests with a 27-inch slope length and three different charge weights.

2. To extend the study of the behavior and path of the rarefaction wave that forms when the shock wave first reaches the top of the slope by the use of a sequence of slope length increases.

The highest HOB, 51 inches above the valley floor, was determined from previous work at URS[1] which indicated that the overpressure at the last station would be predictable from standard flat-terrain HOB curves, i.e. 2W fall-off curves.

The lowest HOB, 7 inches above the valley floor, was chosen somewhat arbitrarily. It was assumed that a charge placed midway between the top and the bottom of the valley would be the lowest HOB of interest.

The choice of a 30-inch intermediate HOB on which greatest emphasis was placed was based on the following:

1. The preliminary theoretical study indicated that HOB of approximately 30 inches would result in the maximum enhancement of air blast.

2. A similarly scaled HOB had been used in previous work at URS[1] and, thus, comparison of data was relatively easy.

Diagrams showing the charge and gauge locations for each of the tests are presented in Appendix A.

MODEL CONSTRUCTION DETAILS

The test model constructed for this contract is of laminated plywood mounted on a steel frame, and was designed with the following objectives in mind:

_____

1/ See Reference 1.

1. To maintain the gauge-holding portion of the model
    in place throughout the entire test series so that
    changing the model would have little or no effect
    on the pressure measurements

2. To allow the model configurations to be changed
    rapidly and with a minimum of manpower

3. To minimize acceleration effects on the measuring
    gauges caused by shocks traveling through the model
    itself

4. To withstand the anticipated high overpressures (in
    excess of 600 psi near GZ) with little deflection
    and to present a uniform reflecting surface to the
    blast wave

A cross section of the model constructed to fulfill
these requirements is shown in Figure 6, and a photograph of
the completed model is shown in Figure 7. In Figure 6.a,
the parts marked A and B, which contain the measuring stations,
are the strongest. These two parts of the model are constructed
of eight layers of 3/4-inch plywood glued together and perma-
nently bolted to the steel frame. They need not be disturbed
by any change in model configuration, and, thus, uniform gauge
mounting conditions were maintained throughout the test series.
The other parts, C through J, are of lighter construction,
two to four thicknesses of laminated plywood. Although
securely fastened during testing, these parts can be easily
moved to change the model configuration.

For the start of the test series (test situation A from
Table I), the model was assembled in the configuration shown
in Figures 6.a and 7, i.e. a 30-degree V-bottom valley with
9-inch slope lengths. As the series progressed, fill-in
part C was removed to expose a 30-degree V-bottom valley with
18-inch slope lengths (test situation B). Parts D, E, and F
were removed in turn until the 30-degree model with 27-inch
slope lengths and an 18-inch flat bottom was exposed (test
situations C through K).

a. 30-Degree Configuration
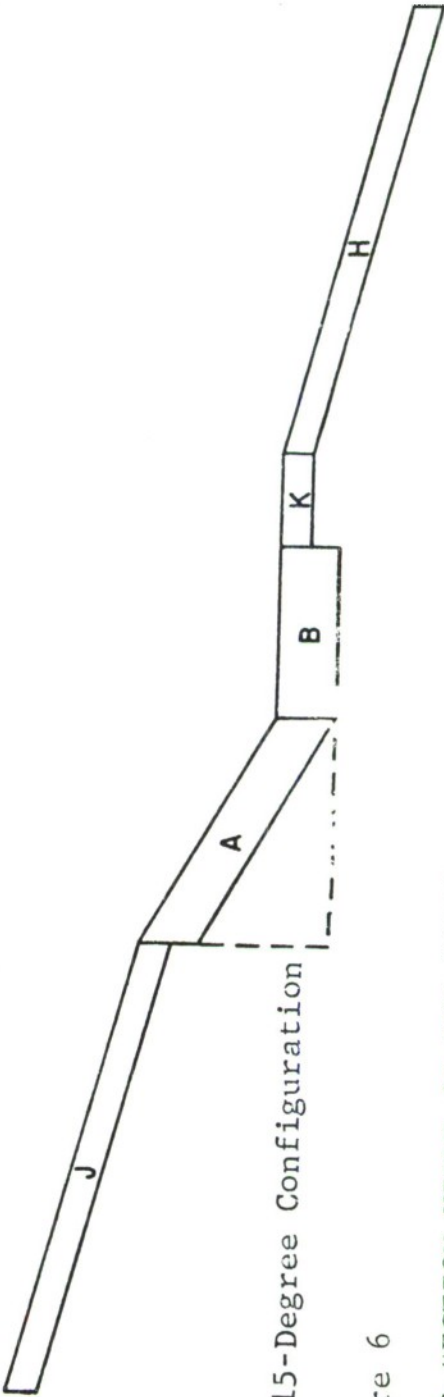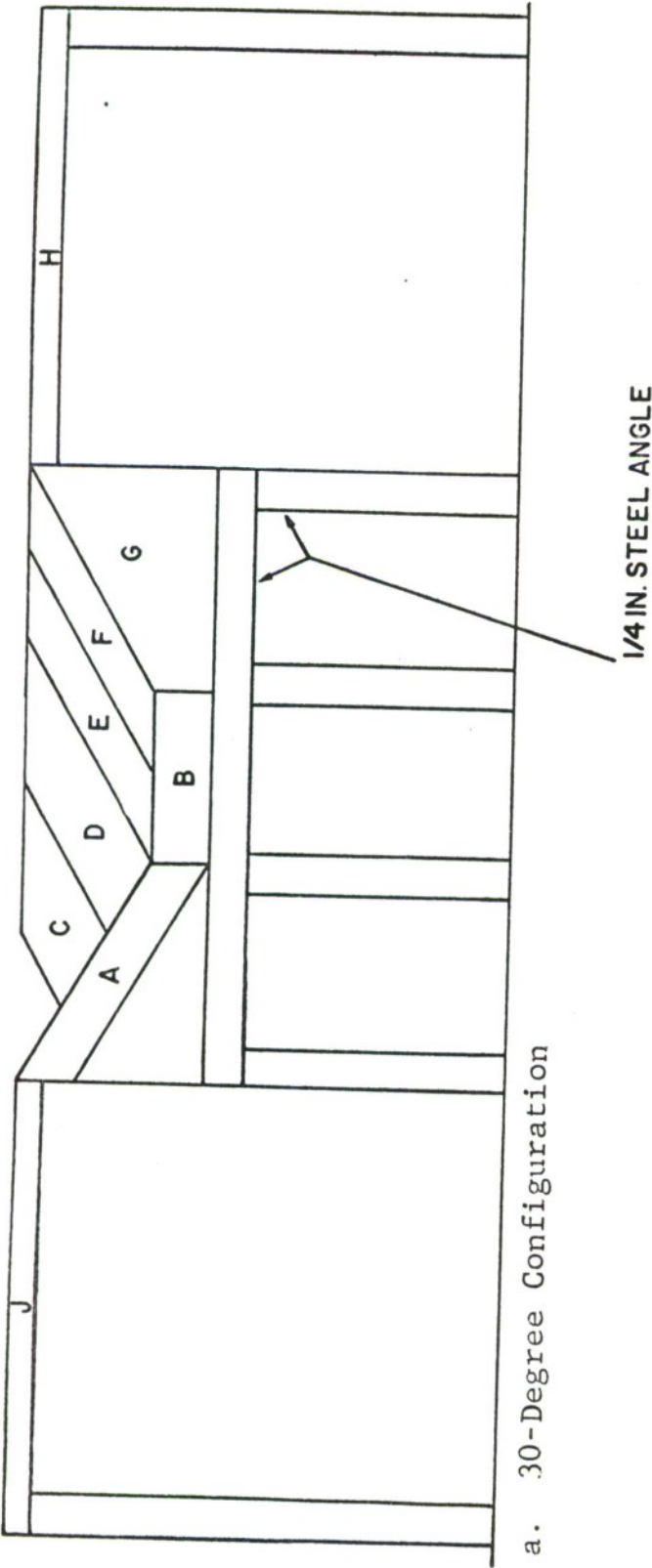
1/4 IN. STEEL ANGLE

b. 15-Degree Configuration

Figure 6

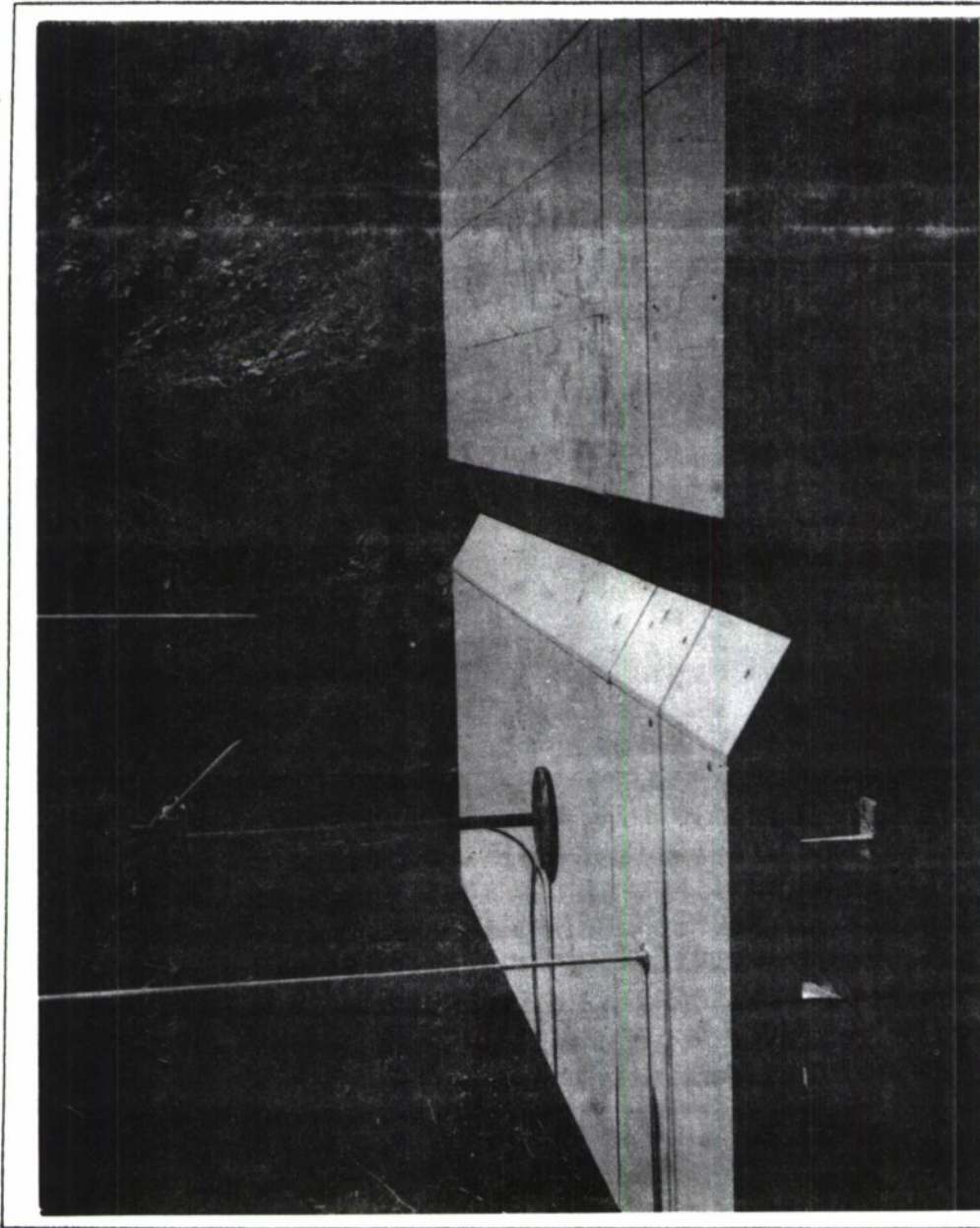CROSS-SECTION VIEWS OF THE MODEL

Figure 7

PHOTOGRAPH OF THE MODEL

For the 15-degree V-bottom valley configuration, parts
A and B with the gauge measuring stations remained in place,
and slope section G was removed. As shown in Figure 6.b, a
flat piece K was installed, and the 4-foot side pieces H and
J were placed at 15 degrees to the horizontal.

The flat-terrain model (test situations M, N, and O) was
constructed by removing part A and placing the 4-foot side
pieces H and J on the same plane as the gauge measuring part
B and the flat fill-in piece K.

The model is divided into two parts at right angles to
the axis of the valley, a 9-foot measuring table and a 3-foot
 charge table. These two tables were isolated from each other
by a 1/2-inch layer of cork. This effectively prevented the
transmission of acceleration shocks from the charge table to
the gauge measuring section.

Measuring System

Two types of air pressure gauges were mounted in the
models used during this project. For the high overpressure
region, over 100 psi, a quartz piezoelectric gauge manufactured
by the Kistler Instrument Company (model 605) was used. For
the lower overpressure region, under 100 psi, a URS piezo-
electric ceramic gauge was used.

The high pressure gauge has a pressure range of 0.5 to
10,000 psi. The electronics used with these gauges consisted
of a model 565 charge amplifier also manufactured by Kistler.

The URS gauges, shown schematically in Figure 8, incorporate
a tube of piezoelectric ceramic (lead zirconate titanite) 1/8
inch long and 1/8 inch in diameter, with a wall thickness of
0.020 inch. The tube, capped by an acetate sheet 0.020 inch
thick, rests on a lucite insulating block. Both are enclosed
in a brass housing. Electrical connections are made by
silver paint and a lead wire soldered to a standard connector.

A gauge to measure air shock pressures in free air, with
internal design similar to the URS gauge, was constructed in
the form of a probe 35 inches long and 1/2 inch in diameter,

0.630 IN. DIA.

0.020 IN. CAP

PIEZOELECTRIC
TUBE

POTTING

SILVER
PAINT

LUCITE
BLOCK

CONNECTING   WIRE

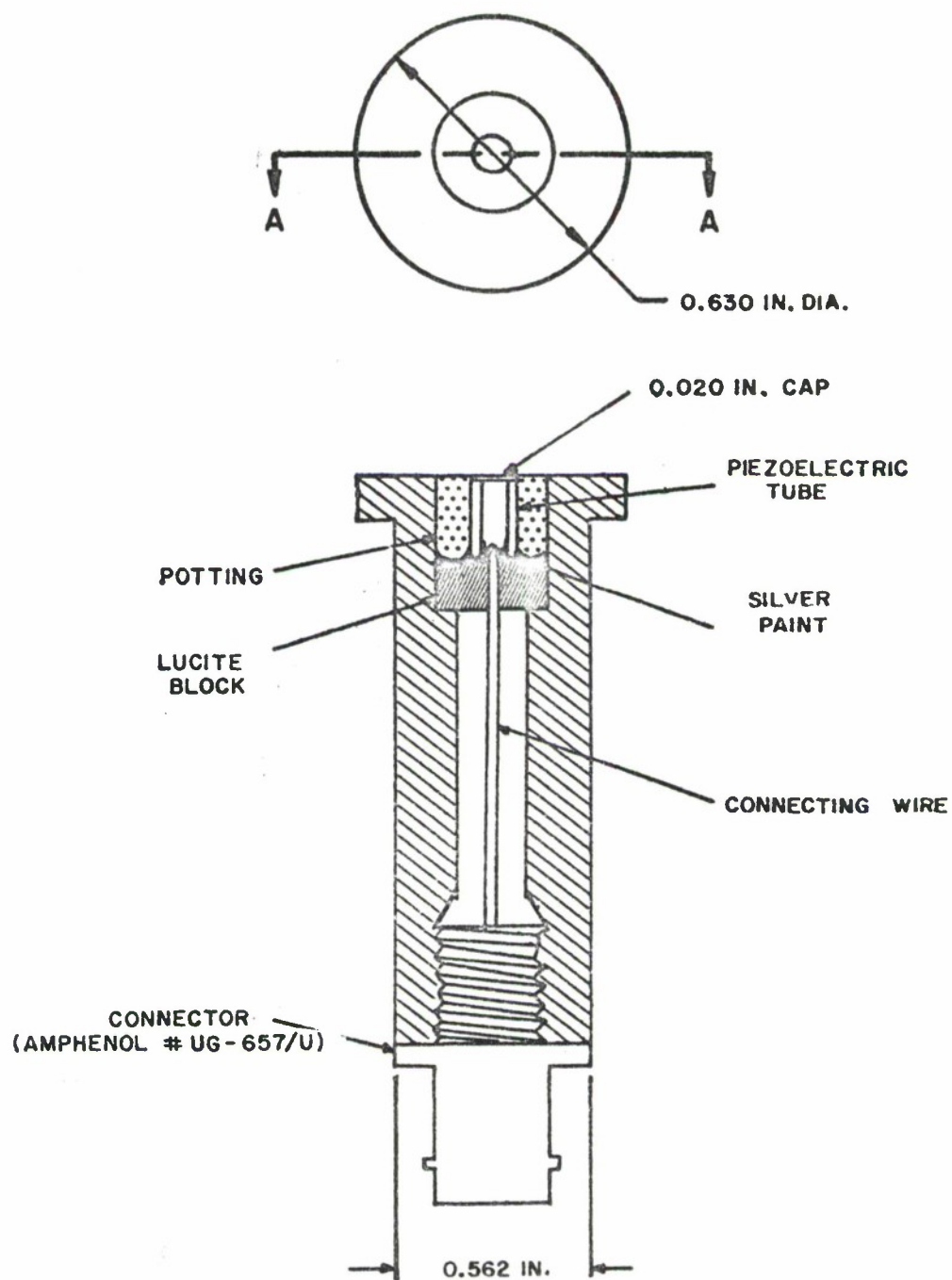CONNECTOR
(AMPHENOL # UG-657/U)

0.562 IN.

Figure 8

SCHEMATIC OF THE TOPOGRAPHY GAUGES

with a pointed end 4 inches long. A 1/8-inch piezoelectric tube mounted in the same manner as in the standard gauges was placed (9 inches) from the pointed end. This probe was mounted about 4 feet above the model on a rigid stand, 3 to 5 feet from the charge, and aimed at its center. The purpose of this gauge was to check on the uniformity and reproducibility of detonation between charges.

The electronics associated with both types of URS gauges consisted of standard cathode-follower type preamplifiers. The recording equipment consisted of dual-beam oscilloscopes equipped with Polaroid cameras. The oscilloscopes were triggered by an additional Kistler quartz gauge located close to GZ and a URS pulse shaping amplifier.

Section IV

TEST RESULTS

The method generally used in determining the magnitude of the effect of a particular valley configuration on air blast is to compare the blast wave characteristics measured at various points in the valley with those obtained on flat terrain for similar detonation conditions. The ratio of peak pressure at a point on the valley surface to peak pressure at a like point the same distance from the charge on flat terrain with the same HOB is termed the amplification factor, and is normally the most important measure of the effect of the valley shape on air blast.

The amplification factors reported herein are all referenced to a HOB measured from the valley floor. It was used in all cases since it is desirable to have a constant reference point for comparison of all data from the scale-model tests and to have one that can be readily used in the field. Usually the most easily obtained and most uniform topographic feature in hilly terrain is the location of the valley floor.

These flat-terrain data have been compared with those from past URS work with the same explosives[1] and with those from work with 250-pound charges[2] as in Figures 9, 10, and 11. Differences were noted, particularly for the 7-inch HOB in the higher pressure regions, some as high as 13 per cent.

Because of these differences, all amplification factors presented in this report are referenced only to the flat terrain data taken during the program.

---

[1]   See Reference 1.

[2]   See Reference 3.
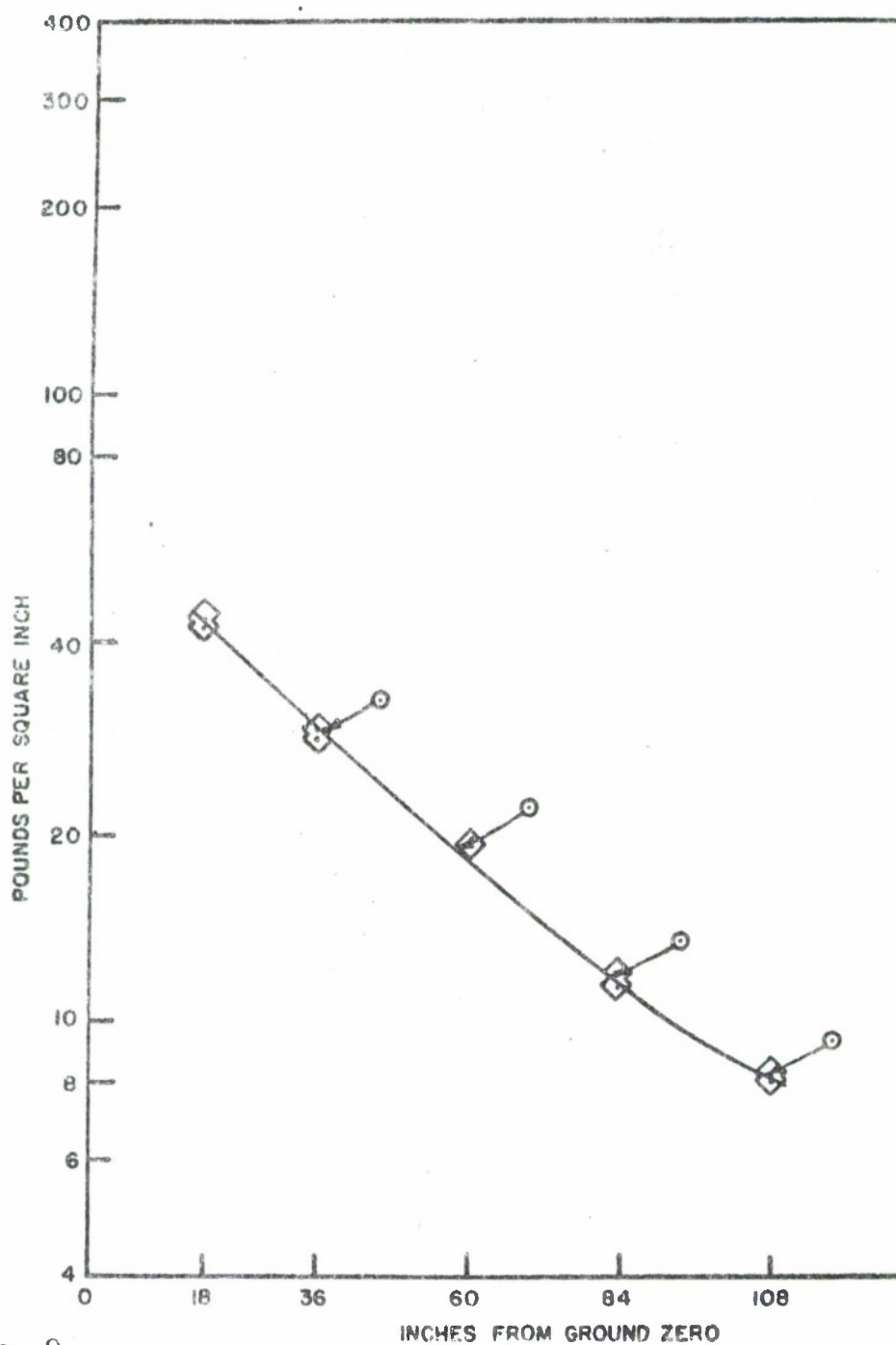
Figure 9

FLAT-TERRAIN DATA FOR 51-INCH HOB

Note: ◇ URS data
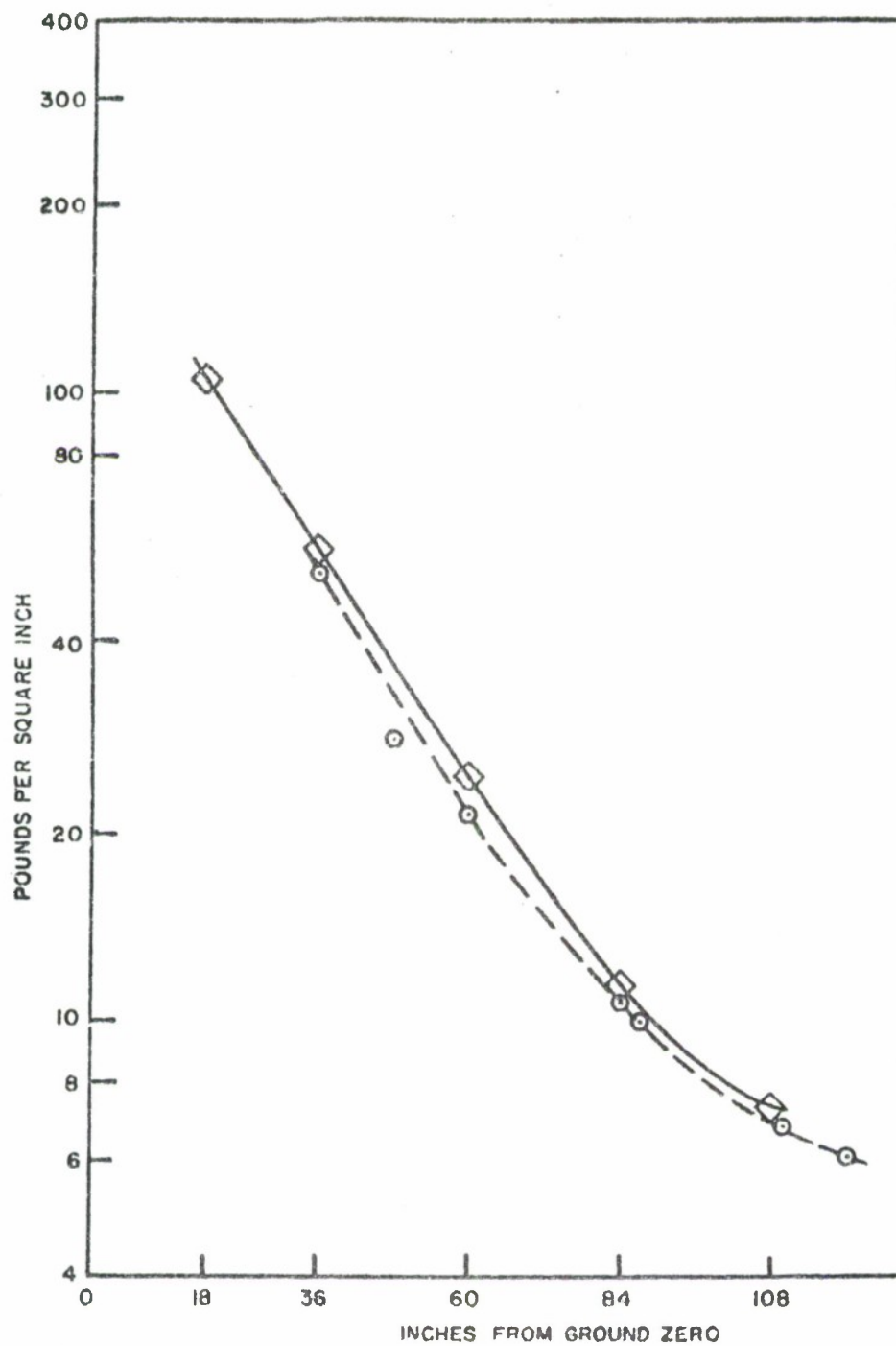   ⊙ Data from References 1 and 3

Figure 10

FLAT-TERRAIN DATA FOR 30-INCH HOB

Note: ◇ URS data
         ⊙ Data from References 1 and 3
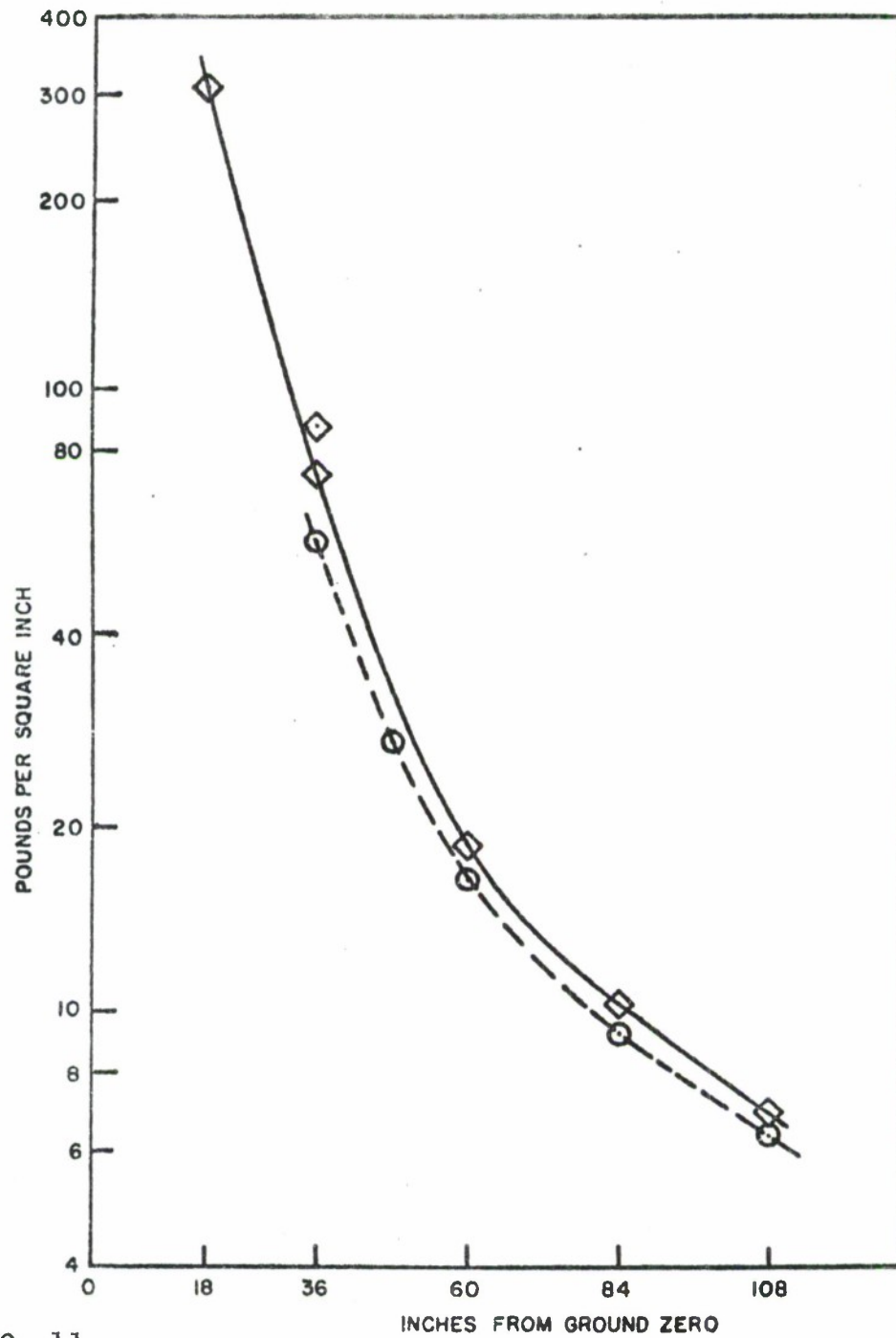
URS 170-

Figure 11

FLAT-TERRAIN DATA FOR 7-INCH HOB

Note: ◇ URS data
   ⊙ Data from References 1 and 3

The peak pressure data obtained from this study is presented in Appendix B. A summary of data measured at the bottom of the various generalized valley models is presented in Figures 12 and 13. The measured peak over-pressure values have been converted to amplification factors by dividing the peak overpressure at a particular distance from GZ in the valley by the peak overpressure at the same distance on the flat terrain.

As shown in Figure 12 for bursts 30 inches above the axis of the 30-degree, V-bottomed valley configuration, at 18 inches from ground zero, amplification factors ranged from 2.5 to 3. That is peak overpressures in the valley P_v ranged from 250 to 300 psi as opposed to peak overpressures on flat terrain P_f of 100 psi for the same HOB and distance from GZ. For the same valley configuration where P_f was approximately 55 psi, 36 inches from GZ, amplification factors were between 1.2 and 2 (P_v of between 80 and 110 psi); where P_f was approximately 25 psi, 60 inches from GZ, ampli-fication factors were between 1.3 and 1.5 (P_v of between 32 and 36 psi).

At greater distances from ground zero, the flat-bottomed valleys, probably more closely representative of natural terrain than the V-bottomed valleys, yielded greater amplification factors. In the flat-bottomed valleys where P_f was about 11 psi, at a distance of 84 inches from GZ, amplification factors of between 1.6 and 1.8 (P_v between 17 and 20 psi) were observed, and where P_f was about 7 psi, at a distance of 108 inches, amplification factors of between 1.5 and 1.6 (P_v between 10 and 12 psi) were observed.

In the 15-degree valley (curve 1 of Figure 12), the maximum amplification factor, 1.4, occurred where P_f was 12 psi, at the 84-inch distance.

For bursts at 51 inches above the 30-degree V-bottomed valley (curve 7 of Figure 12), at the closest station where P_f was 42 psi, the amplification factor was about 1.8 (P_v = 76 psi), and at the furthest station where P_f was 8 psi, the amplification factor was 1.0, i.e. valley and flat-terrain

DISTANCE FROM GROUND ZERO (IN.)
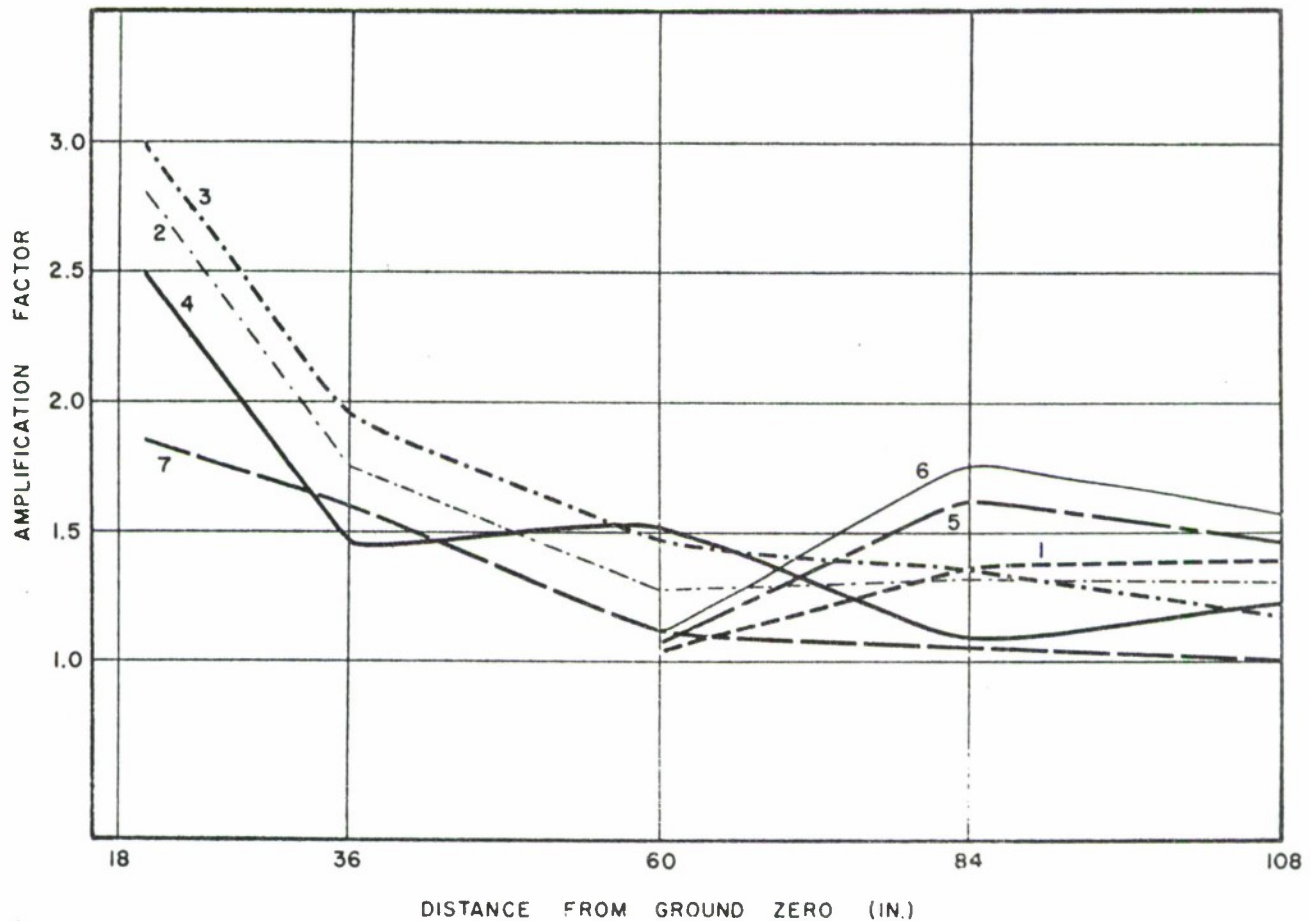
Curve	HOB (inches)	Test Geometry
1	30	27-in. V-valley 15-deg
2	30	27-in. V-valley 30-deg
3	30	18-in. V-valley 30-deg
4	30	9-in. V-valley 30-deg
5	30	27-in. 18-in. Flat-bottom Valley 30-deg
6	30	27-in. 9-in. Flat-bottom Valley 30-deg
7	51	27-in. V-valley 30-deg

Figure 12

AMPLIFICATION FACTOR VERSUS DISTANCE FROM GROUND ZERO
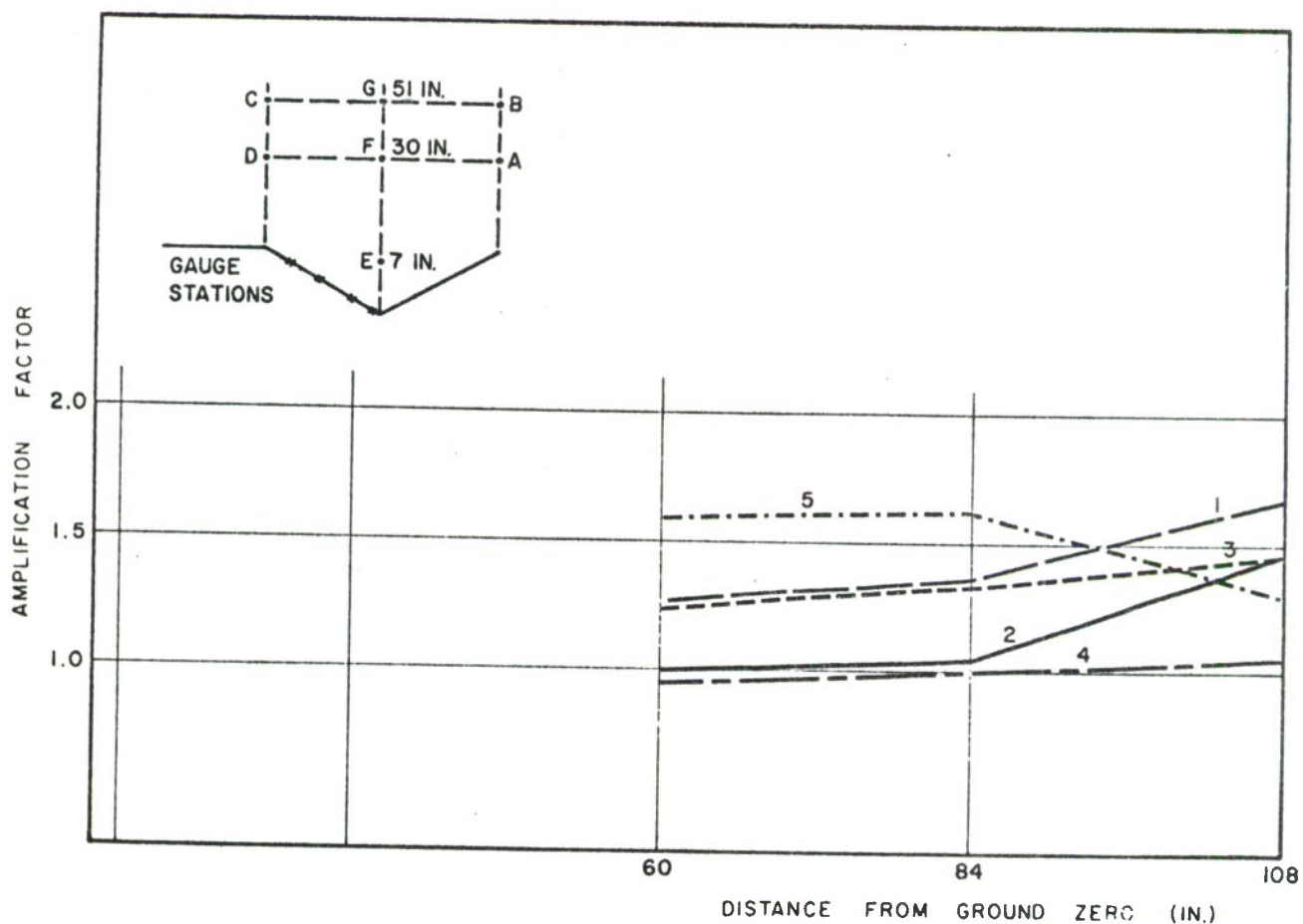
Curve	HOB (inches)	Charge Location	Test Geometry
1	30	A	27-in. V-valley 30-deg
2	30	D	27-in. V-valley 30-deg
3	51	B	27-in. V-valley 30-deg
4	51	C	27-in. V-valley 30-deg
5	7	E	27-in. V-valley 30-deg

Figure 13

AMPLIFICATION FACTOR VERSUS DISTANCE FROM GROUND ZERO

pressures were identical. This result had been anticipated from previous work at URS[1] and indeed had provided a basis for using the 51-inch HOB in this program.

For the 7-inch HOB in which the charge was within the valley (curve 5 of Figure 13), where P_f was 20 and 10 psi at distances of 60 and 84 inches from GZ, amplification factors were 1.6 and 1.7, respectively (P_v = 32 and 17 respectively).

In tests in which explosions took place above the edges of the valleys rather than above their center lines, amplification factors were observed to increase with distance from the charge, with the largest factors being measured at the most distant stations. The highest amplification factors 1.4 and 1.7 were observed when the charge was above the lip of the valley opposite the measuring stations (curves 1 and 3 of Figure 13).

A few tests were conducted with the URS dynamic pressure (Q) gauge to determine feasibility of its use in making measurements in some of the valley shapes. Records from these tests indicate that it will be possible to make dynamic pressure measurements in the flat-bottom valley.

---

[1]   See Reference 1.

Section V

CONCLUSIONS AND RECOMMENDATIONS

This study has demonstrated that significant channeling of air blast does occur in a large number of the generalized valley shapes tested. It must be emphasized, however, that the primary objective of this study was to determine whether significant channeling could occur, and its magnitude. This dictated an approach in which as many valley and charge parameters as possible were sampled within the limited scope of the program, without attempting to make a complete study of any one specific condition. The raw data obtained during this contract have been analyzed for peak pressure information, time was not available to acquire pressure-time information or to determine possible rarefaction patterns.

Thus, while the trends indicated in this report are valid, any extrapolation to full-scale situations should await further analysis of data and further experimental tests, which should include:

1.   Additional testing on those valley shapes that have yielded the greatest amplification of air blast

2.   A more comprehensive analysis of the data to obtain pressure-time information

3.   Testing of other generalized valley shapes of tactical interest including converging valleys, and valleys with closed ends

LIST OF REFERENCES

1. A. B. Willoughby, K. Kaplan, and R. Condit. <u>Effects of Topography on Shock Waves in Air</u>, AFSWC-TR-57-9. Burlingame, California: Broadview Research Corporation, August 1956. Confidential.

2. R. Courant and K. O. Friedrichs. <u>Supersonic Flow and Shock Waves</u>. New York: Interscience Publishers, 1948.

3. J. D. Shreve, Jr. <u>Pressure-Distance-Height Study of 250-lb TNT Spheres</u>, AFSWP-WT-520. Albuquerque, New Mexico: Sandia Corporation, March 1953.
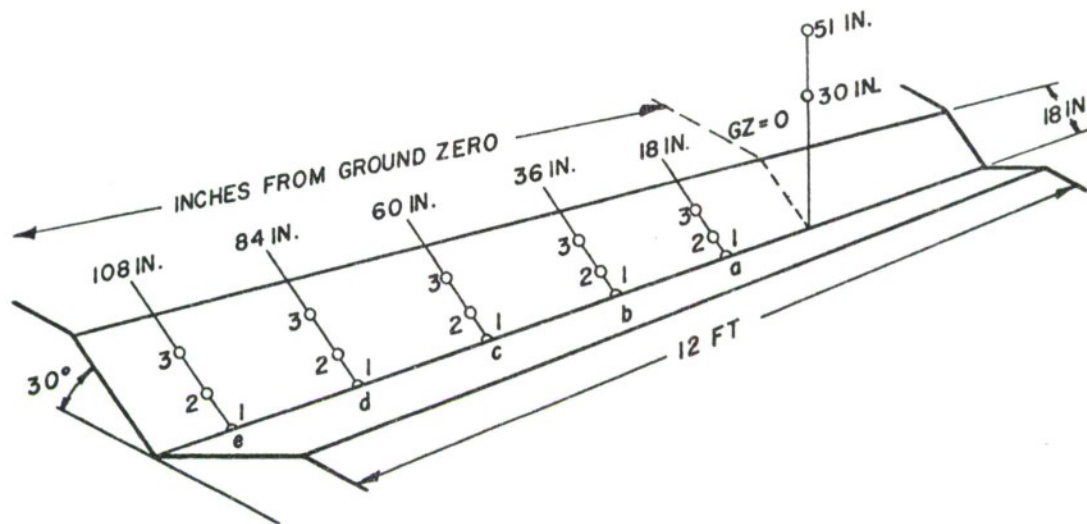
Appendix A

DIAGRAMS SHOWING THE CHARGE AND GAUGE LOCATIONS
FOR EACH OF THE TESTS
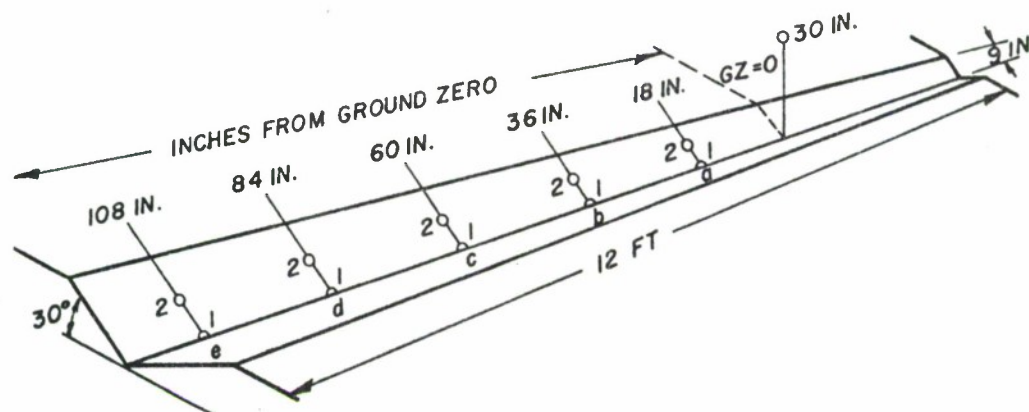
Shot	HOB	Gauge Stations				
		a-18	b-36	c-60	d-84	e-108
Number	(inches)	Inches	Inches	Inches	Inches	Inches
1	30	1,2	1,2	1,2	1	1
2	30	1,2	1,2	1,2	2	2

Figure 14

LOCATION OF INSTRUMENTED GAUGE STATIONS FOR THE 9-INCH
V-BOTTOM 30-DEGREE VALLEY TESTS

		Gauge Stations				
Shot Number	HOB (inches)	a-18 Inches	b-36 Inches	c-60 Inches	d-84 Inches	e-108 Inches
3	30	1,3	1,3	1,3	1,3	
4	30	1,3	1,3	2	2	1,3
5	30			1,2,3	1,2,3	1,3

Figure 15
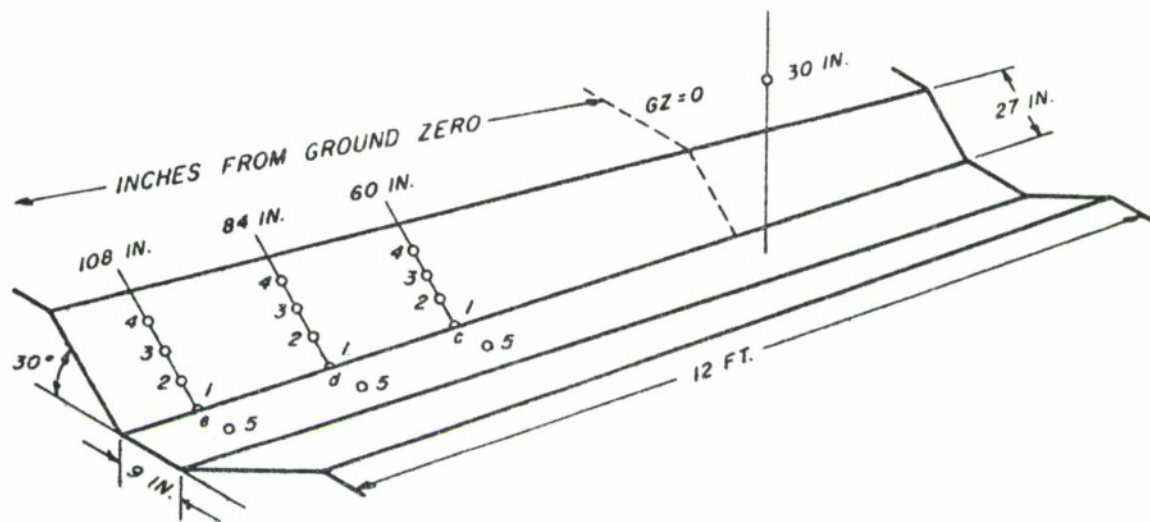
LOCATION OF INSTRUMENTED GAUGE STATIONS FOR THE 18-INCH
V-BOTTOM 30-DEGREE VALLEY TESTS
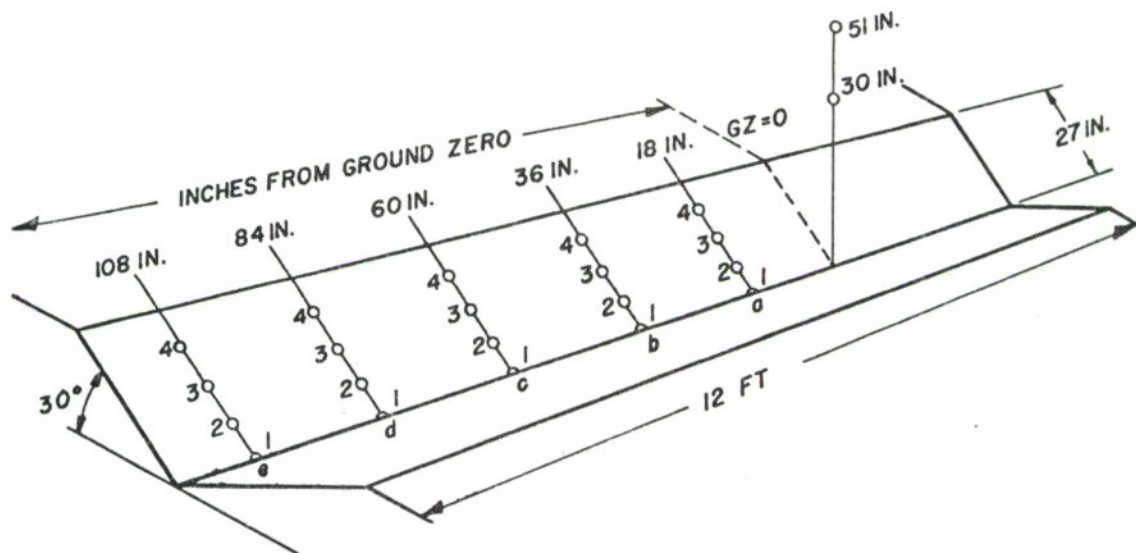
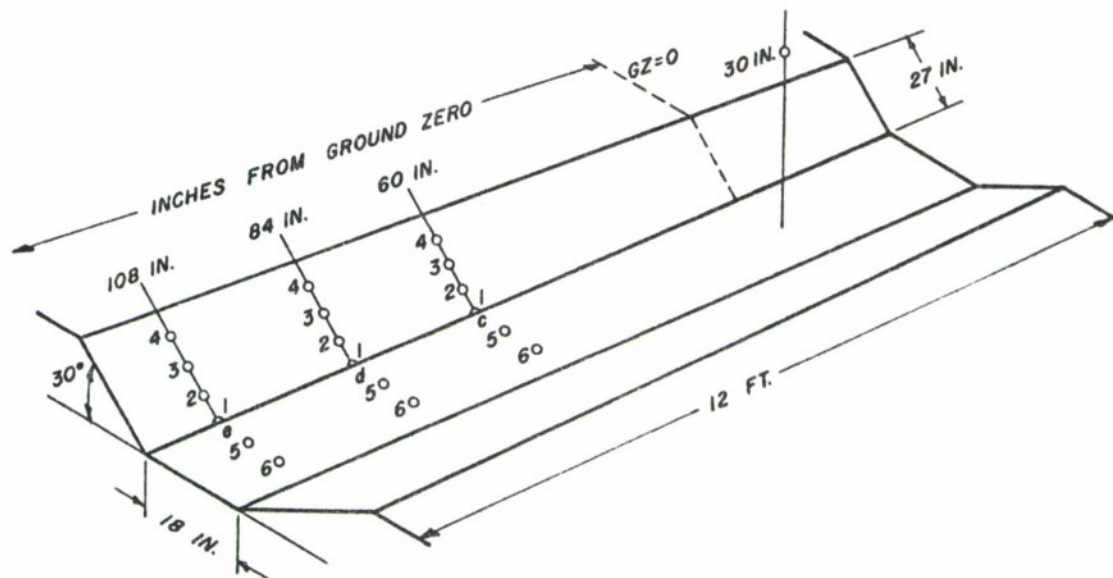|		Gauge Stations				
Shot Number	HOB (inches)	a-18 Inches	b-36 Inches	c-60 Inches	d-84 Inches	e-108 Inches
6	30			1,4	1,3,4	1,3,4
7	30	1,4	1,4		3	1,3,4
8	30	1,4	1,4	1,4	1,4	
9	51	1,4	1,4	1,4	1,4	
10	51	1,4	1,4	3	3	1,3

Figure 16

LOCATION OF INSTRUMENTED GAUGE STATIONS FOR THE 27-INCH
V-BOTTOM 30-DEGREE VALLEY TESTS
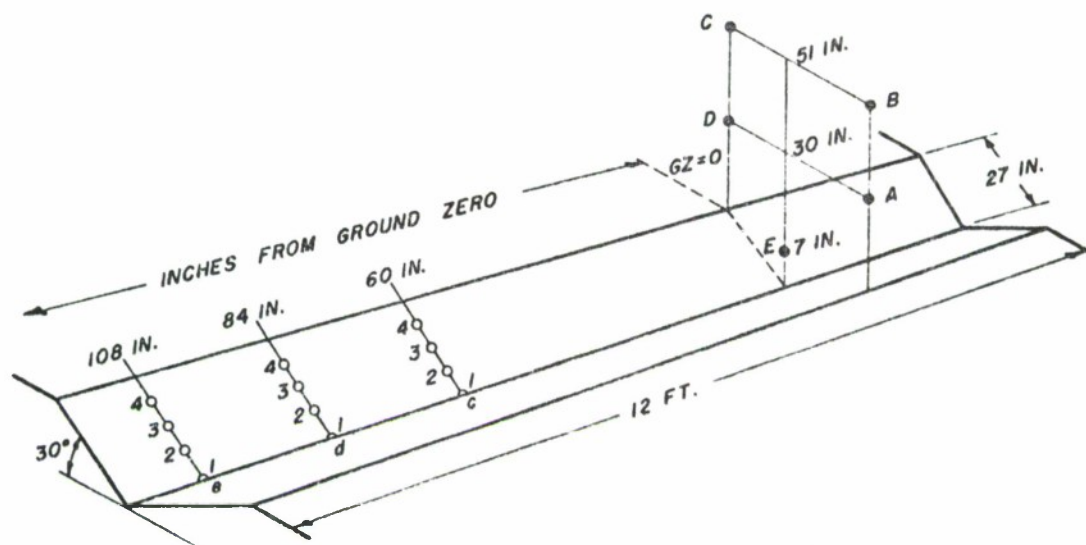
Shot Number	HOB (inches)	Charge Location	Gauge Stations c-60 Inches	d-84 Inches	e-108 Inches
12	51	C	1,2,3,4	1,2,3,4	
13	51	C		1,2,3,4	1,2,3,4
14	51	C	1,2,3,4		1,2,3,4
15	51	B	1,2,3,4	1,2,3,4	
16	51	B		1,2,3,4	1,2,3,4
17	51	B	1,2,3,4		1,2,3,4
18	30	A	1,2,3,4	1,2,3,4	
19	30	A		1,2,3,4	1,2,3,4
20	30	A	1,2,3,4		1,2,3,4
21	30	D	1,2,3,4	1,2,3,4	
22	30	D		1,2,3,4	1,2,3,4
23	30	D	1,2,3,4		1,2,3,4
24	7	E	1,2,3,4	1,2,3,4	
25	7	E		1,2,3,4	1,2,3,4
26	7	E	1,2,3,4		1,2,3,4

Figure 17

LOCATION OF INSTRUMENTED GAUGE STATIONS FOR THE 27-INCH
V-BOTTOM 30-DEGREE VALLEY TESTS

Shot Number	HOB (inches)	Gauge Stations		
		c-60 Inches	d-84 Inches	e-108 Inches
27	30	1,3,4,5	1,3,4,5	
28	30		1,3,4,5	1,3,4,5
29	30	1,3,4,5		1,3,4,5

Figure 18

LOCATION OF INSTRUMENTED GAUGE STATIONS FOR THE 9-INCH
FLAT-BOTTOM 30-DEGREE VALLEY TESTS

Shot Number	HOB (inches)	Gauge Stations		
		c-60 Inches	d-84 Inches	e-108 Inches
30	30	1,2,3,4,5,6	1,3	
31	30		4,5,6	1 3,4,5,6
32	30	1,2,3,4,5,6	1,3	
33	30		4,5,6	1,3,4,5,6

Figure 19

LOCATION OF INSTRUMENTED GAUGE STATIONS FOR THE 18-INCH
FLAT-BOTTOM 30-DEGREE VALLEY TESTS
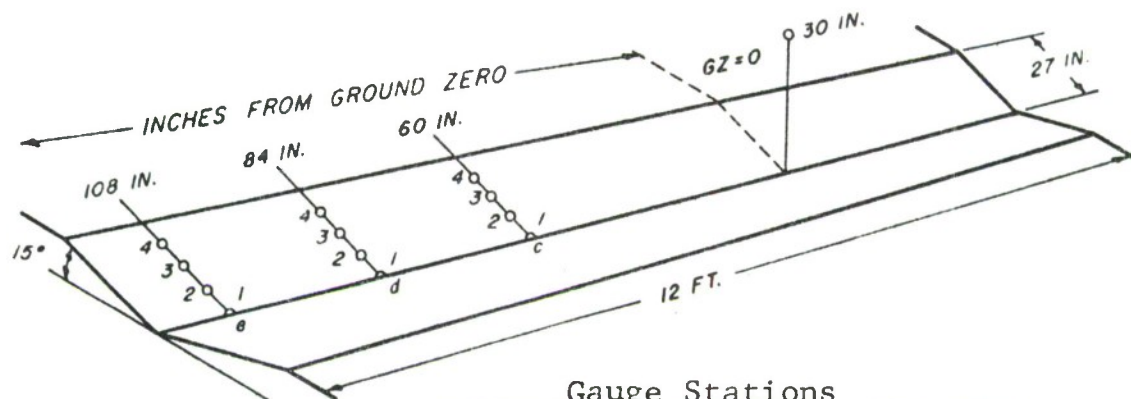
Shot Number	HOB (inches)	Gauge Stations		
		c-60 Inches	d-84 Inches	e-108 Inches
34	30	1,2,3,4	1,2,3,4	
35	30		1,2,3,4	1,2,3,4
36	30	1,2,3,4		1,2,3,4

Figure 20

LOCATION OF INSTRUMENTED GAUGE STATIONS FOR THE 27-INCH
V-BOTTOM 15-DEGREE VALLEY TESTS

Appendix B

PEAK PRESSURE DATA

The following pressure-distance curves pre-
sent the peak pressure data recorded during
the experimental portion of this study. All
points, plotted by location on the valley
slope, represent the average value of at
least two records. The broken lines are
flat-terrain reference curves obtained dur-
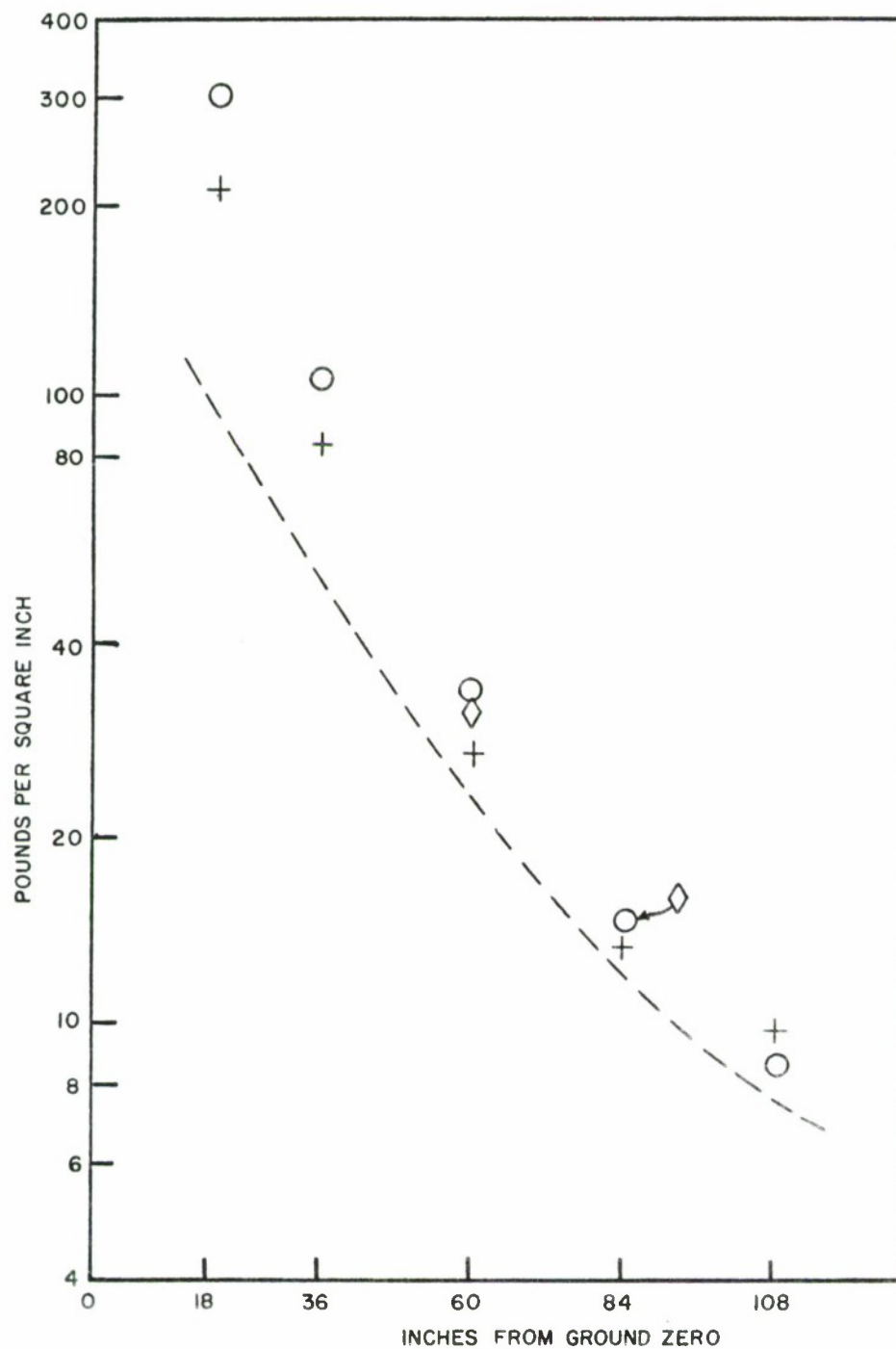ing this program and are presented for com-
parison purposes.
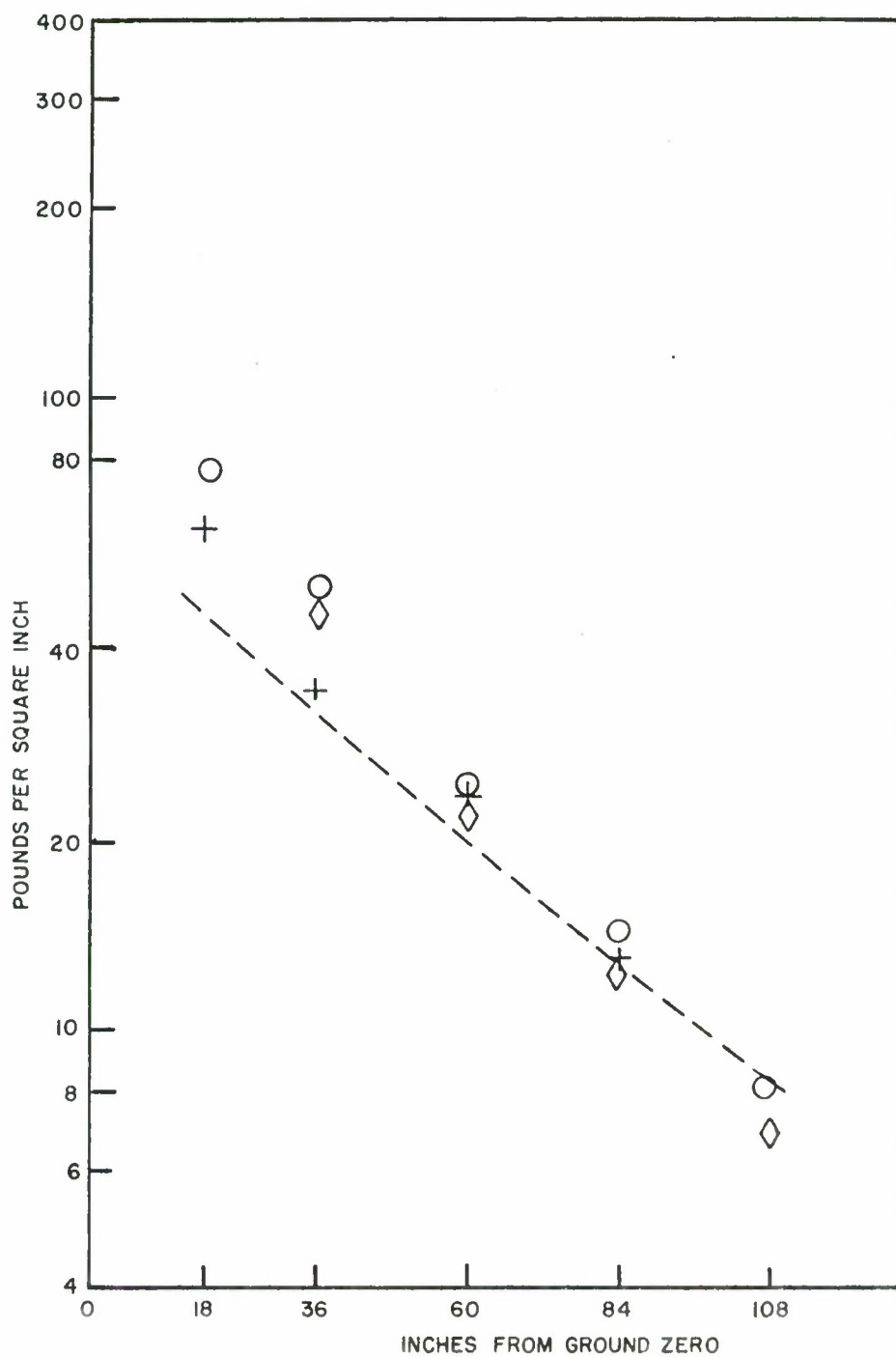
Figure 21

PEAK PRESSURE DATA FOR 51-INCH HEIGHT OF BURST 27-INCH
V-BOTTOM VALLEY BURST ON AXIS

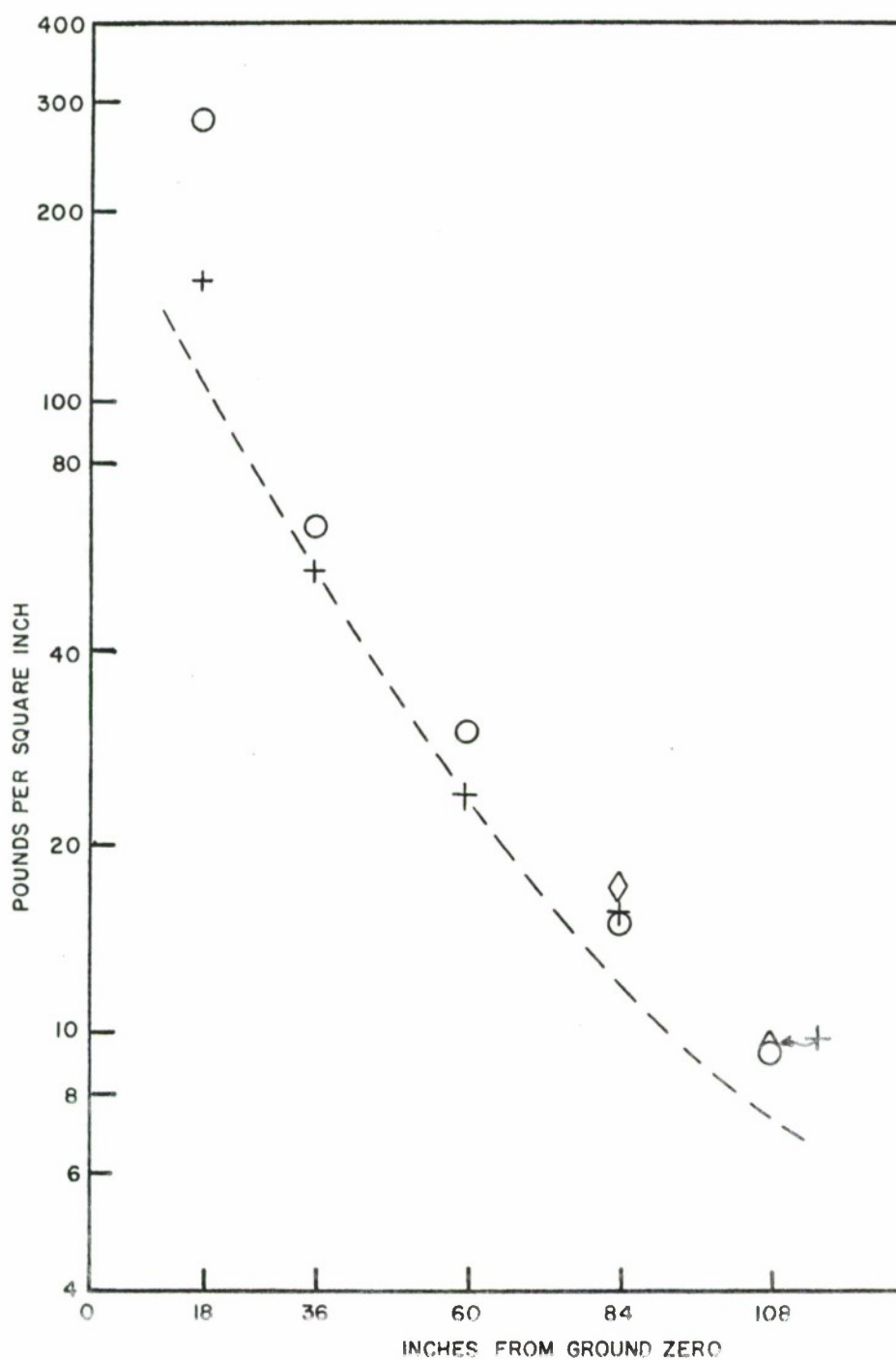+ Top of Slope   ◊ Middle of Slope

O Bottom of Slope   ✕ Near the Bottom of Slope
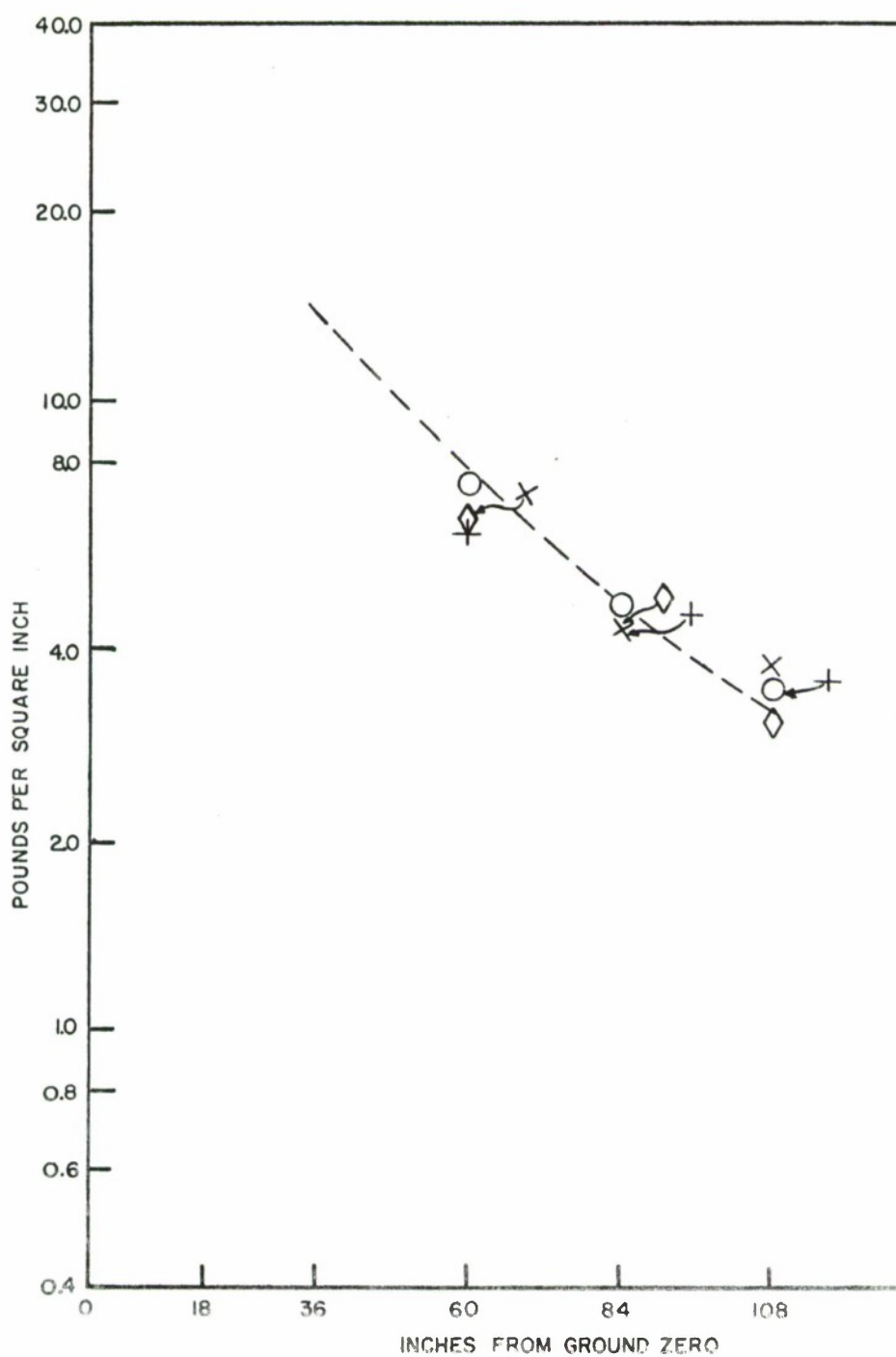
Figure 22

PEAK PRESSURE DATA FOR 51-INCH HEIGHT OF BURST 27-INCH
V-BOTTOM VALLEY BURST ON LEFT SIDE

+ Top of Slope   ○ Bottom of Slope
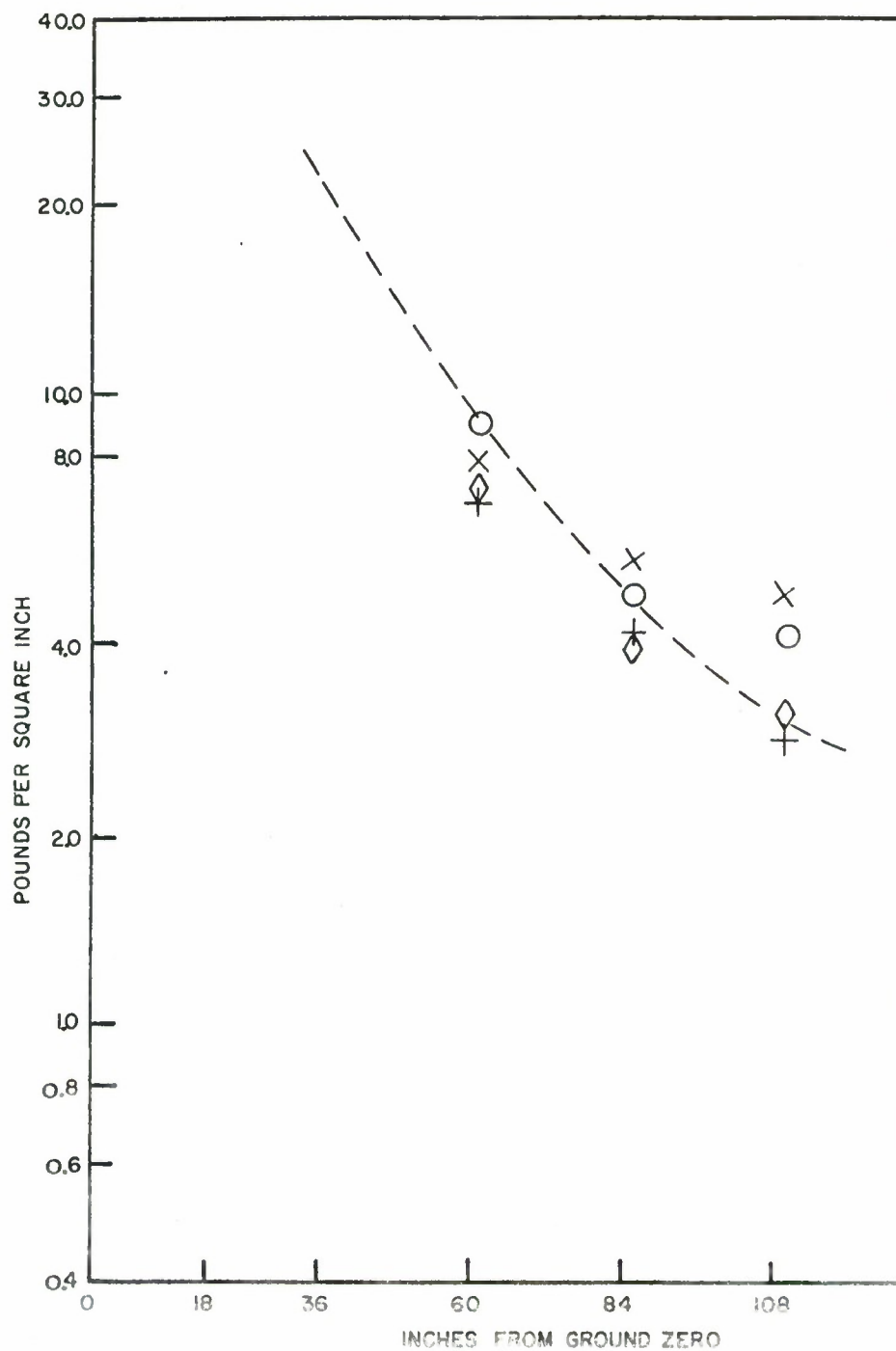◇ Middle of Slope   ✕ Near the Bottom of Slope
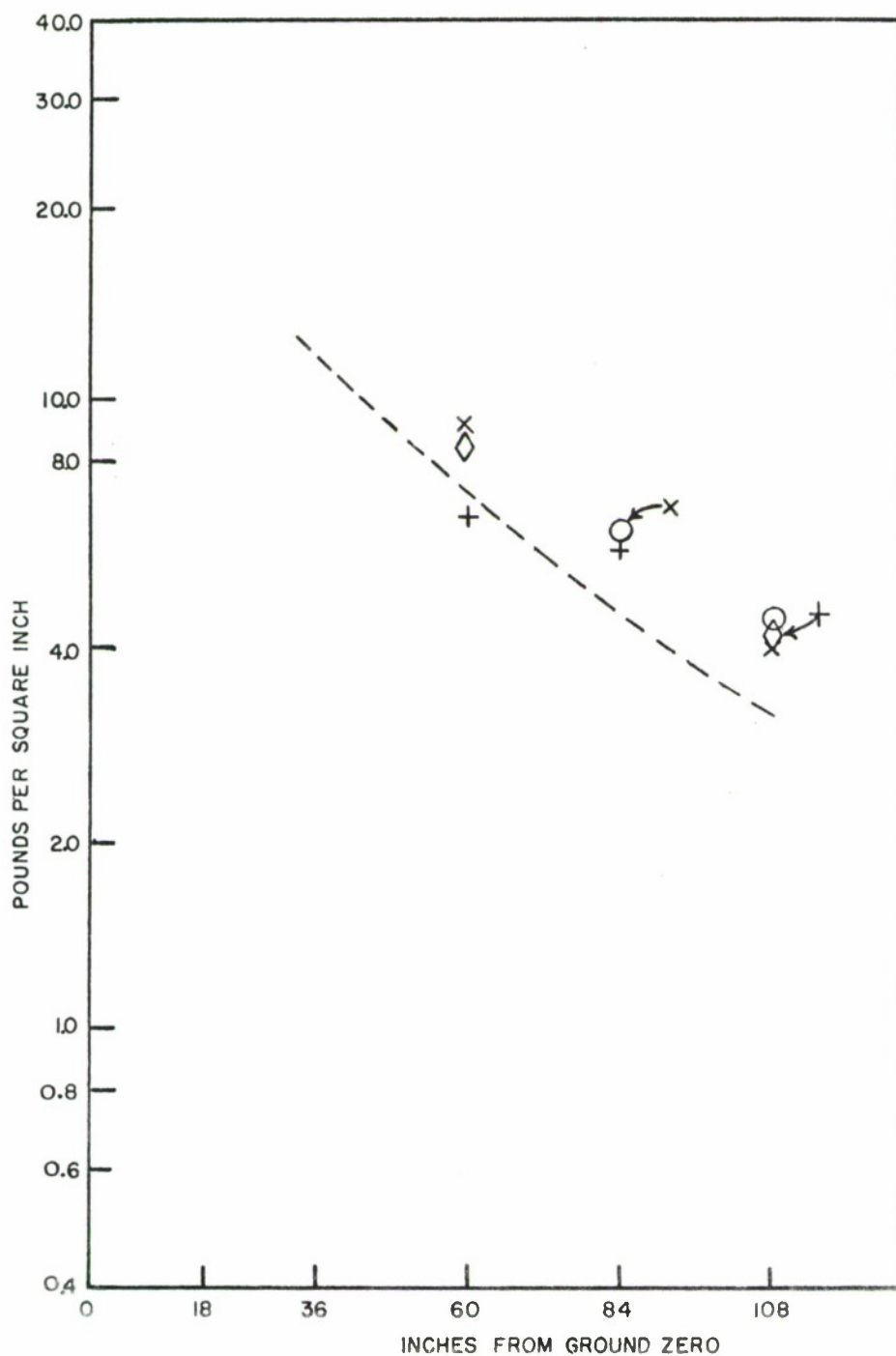
Figure 23

PEAK PRESSURE DATA FOR 51-INCH HEIGHT OF BURST 27-INCH
V-BOTTOM VALLEY BURST ON RIGHT SIDE

+ Top of Slope   ◇ Middle of Slope
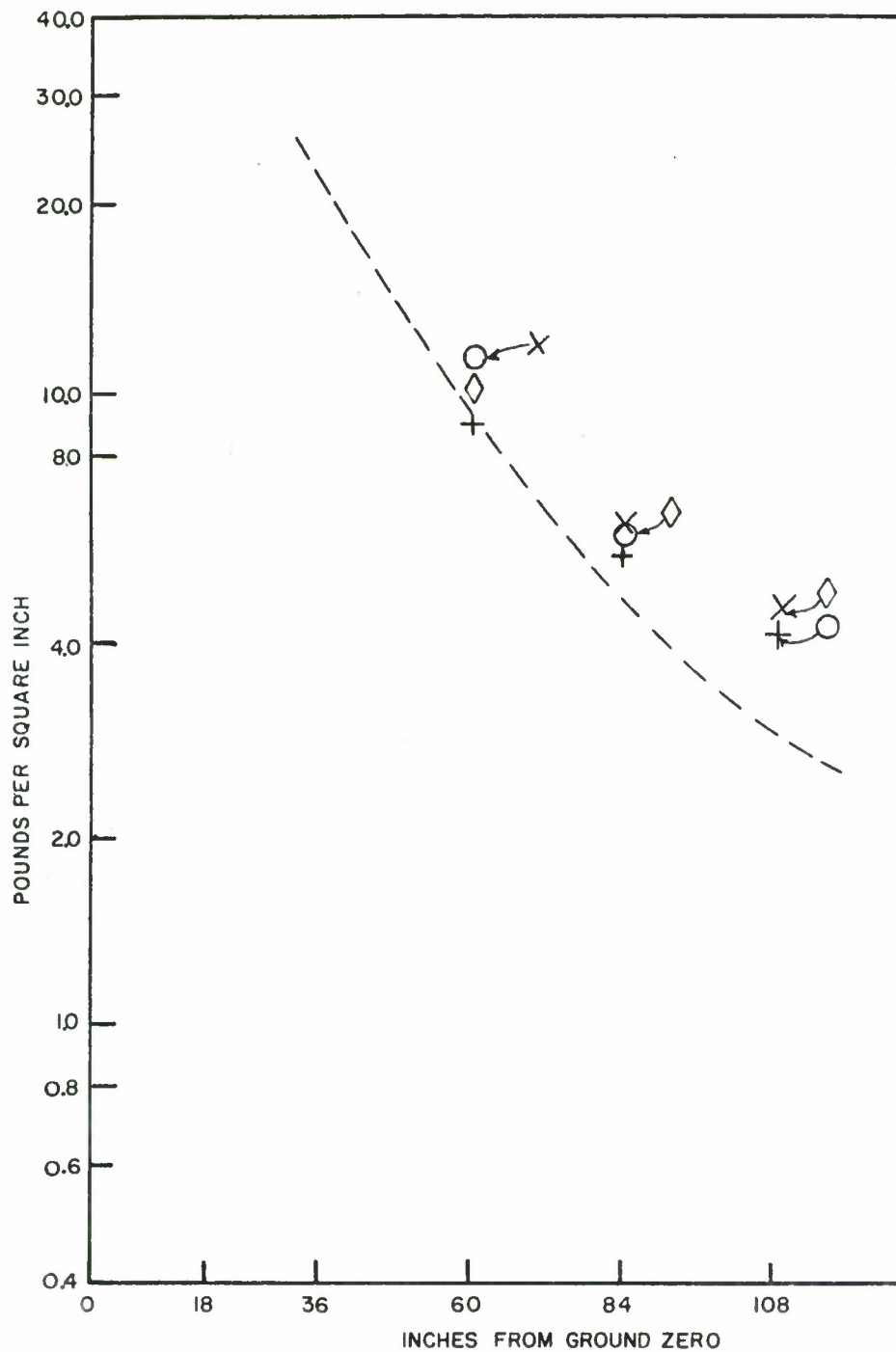O Bottom of Slope   X Near the Bottom of Slope
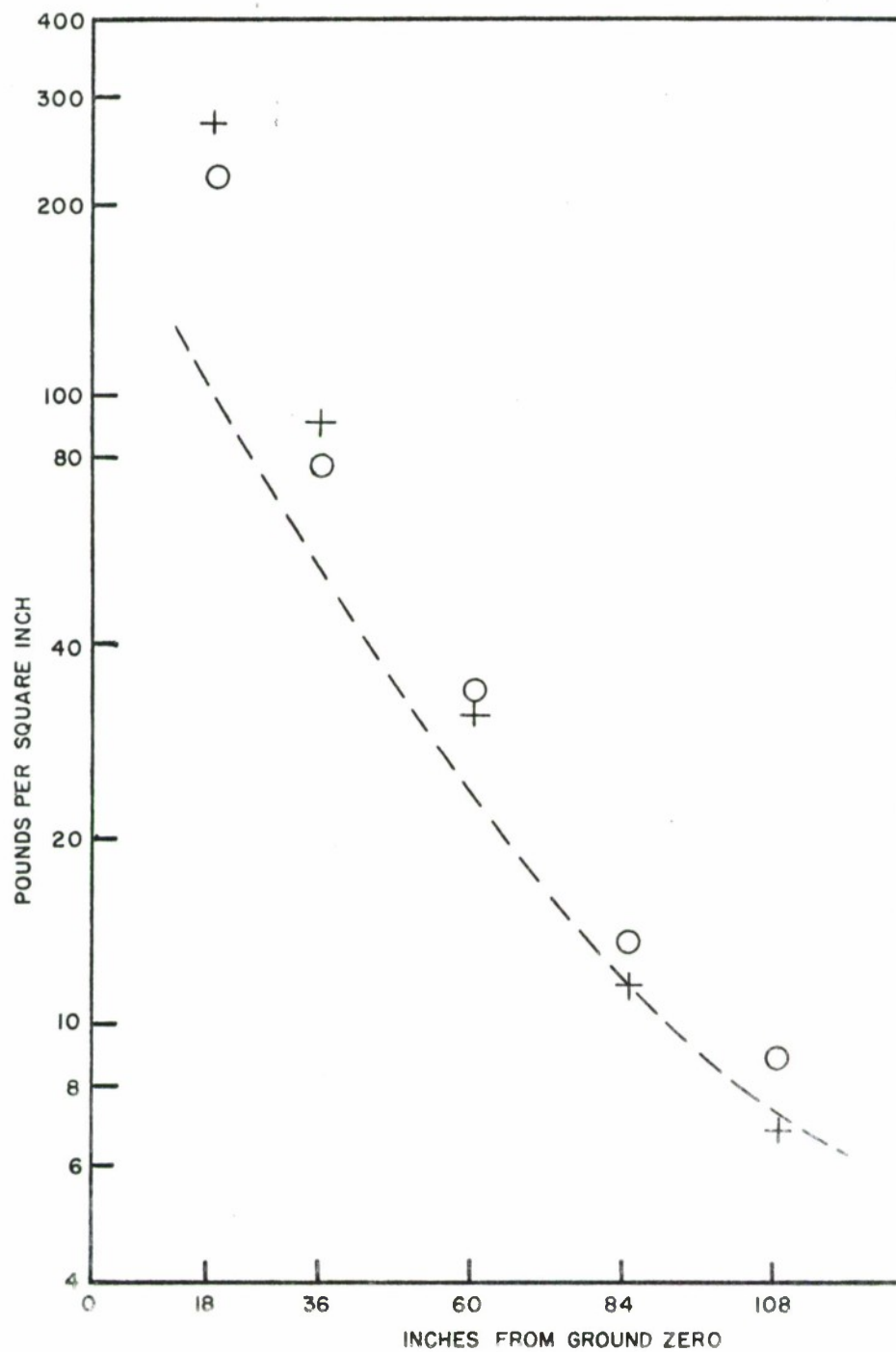
Figure 24

PEAK PRESSURE DATA FOR 30-INCH HEIGHT OF BURST 9-INCH
V-BOTTOM VALLEY BURST ON AXIS

+ Top of Slope   O Bottom of Slope

Figure 25

PEAK PRESSURE DATA FOR 30-INCH HEIGHT OF BURST 18-INCH
V-BOTTOM VALLEY BURST ON AXIS

+ Top of Slope   ◇ Middle of Slope

O Bottom of Slope

Figure 26

PEAK PRESSURE DATA FOR 30-INCH HEIGHT OF BURST 27-INCH
V-BOTTOM VALLEY BURST ON AXIS

+ Top of Slope   ◊ Middle of Slope
O Bottom of Slope

Figure 27

PEAK PRESSURE DATA FOR 30-INCH HEIGHT OF BURST 27-INCH
V-BOTTOM VALLEY BURST ON LEFT SIDE

+ Top of Slope   ◇ Middle of Slope
O Bottom of Slope   ✕ Near the Bottom of Slope

Figure 28

PEAK PRESSURE DATA FOR 30-INCH HEIGHT OF BURST 27-INCH
V-BOTTOM VALLEY BURST ON RIGHT SIDE

+ Top of Slope   ◇ Middle of Slope
O Bottom of Slope   ✕ Near the Bottom of Slope
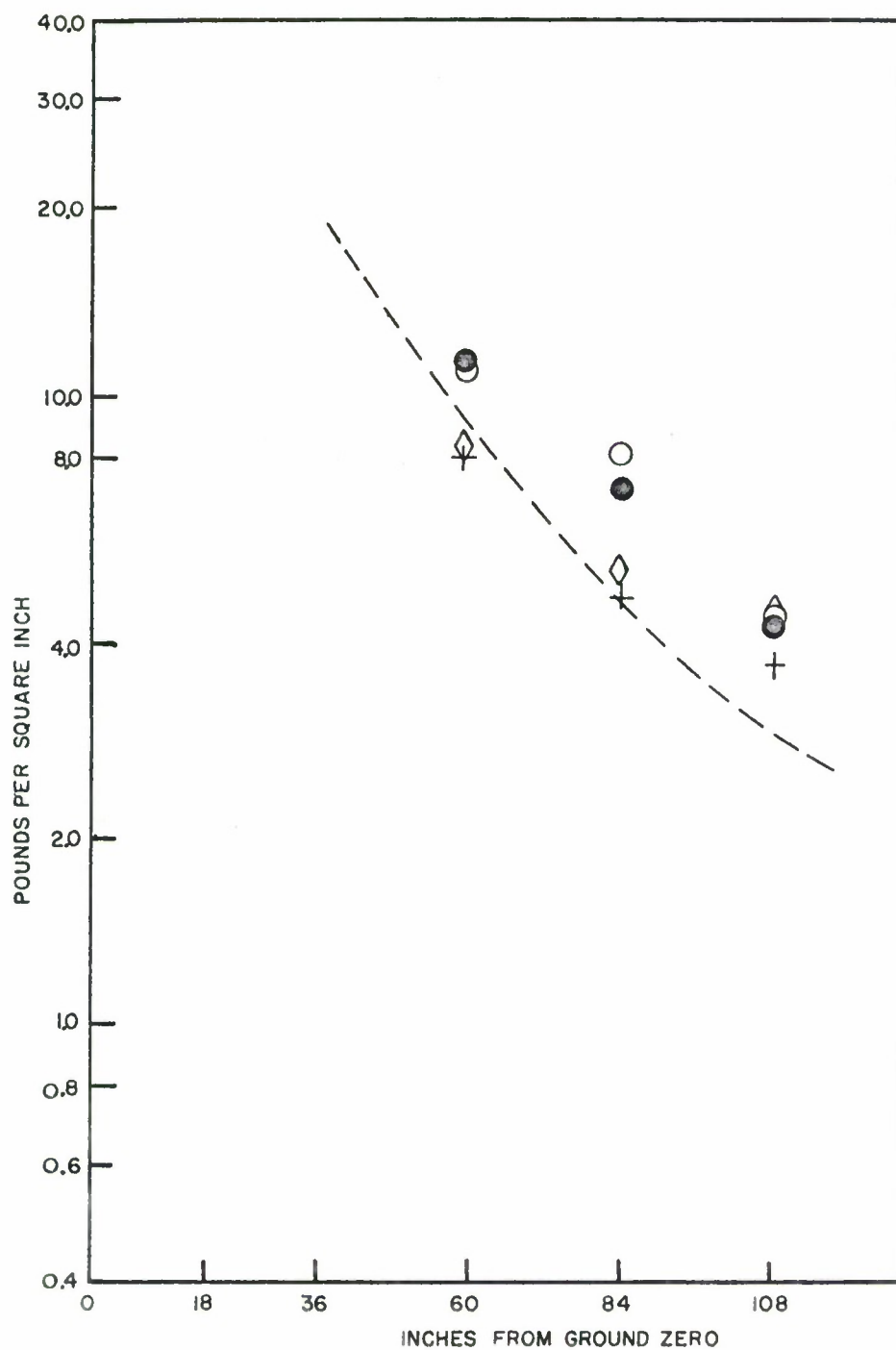
Figure 29

PEAK PRESSURE DATA FOR 30-INCH HEIGHT OF BURST 9-INCH
FLAT-BOTTOM VALLEY

+ Top of Slope   ◇ Middle of Slope
○ Bottom of Slope   ✕ Near the Bottom of Slope
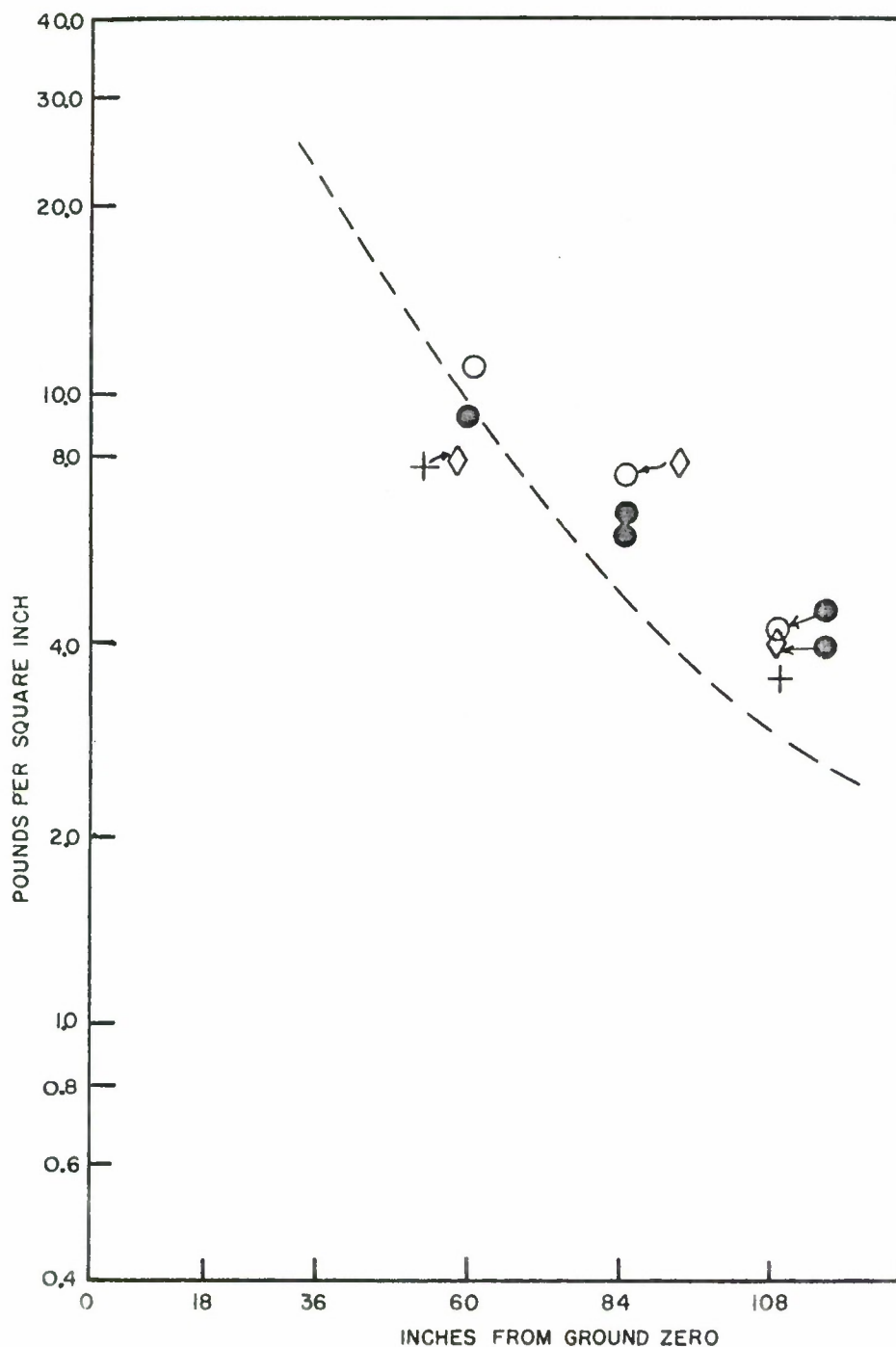● On Flat Bottom

Figure 30

PEAK PRESSURE DATA FOR 30-INCH HEIGHT OF BURST 18-INCH
FLAT-BOTTOM VALLEY

+ Top of Slope   ◊ Middle of Slope
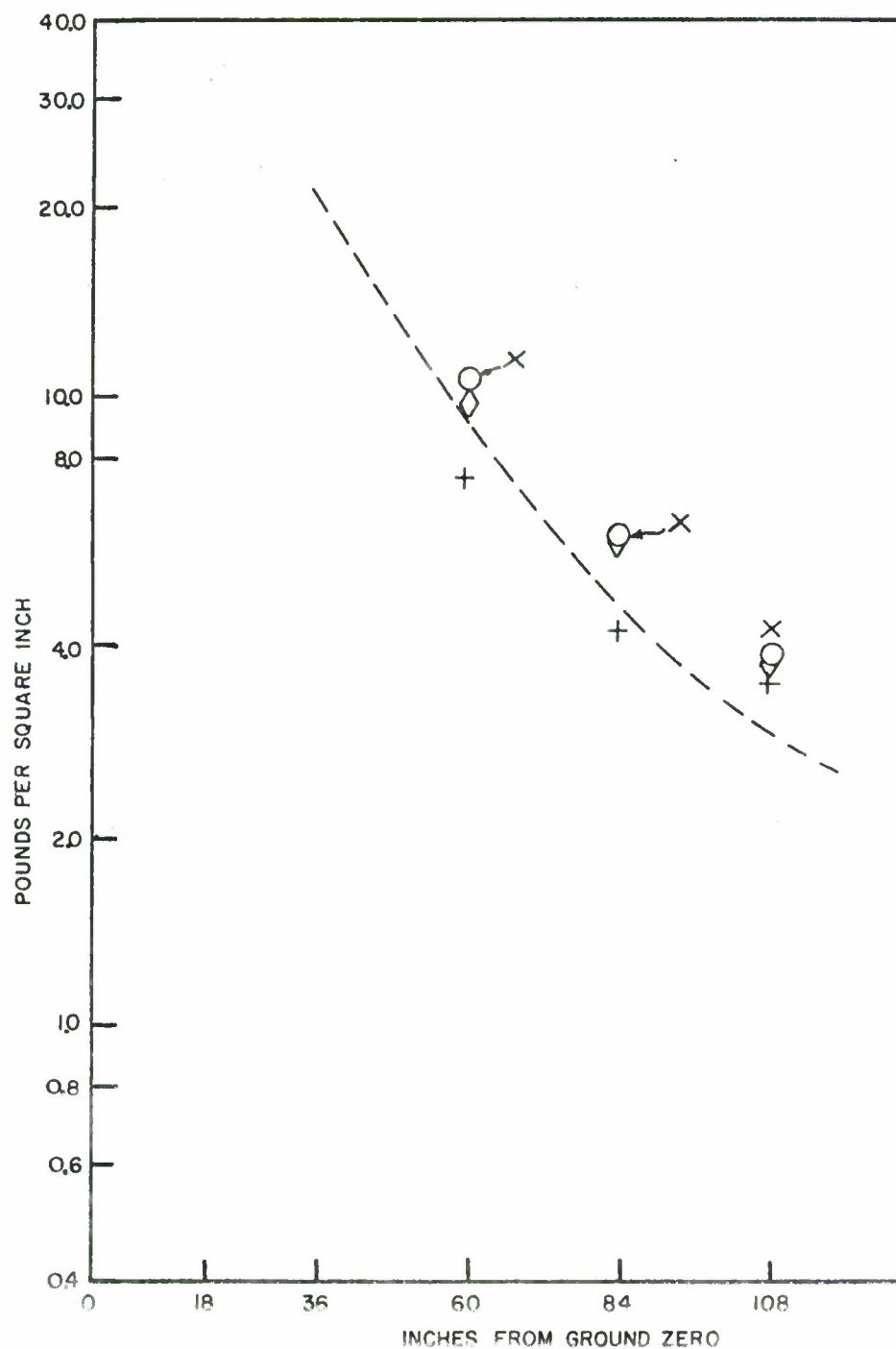○ Bottom of Slope   ● On Flat Bottom

Figure 31

PEAK PRESSURE DATA FOR 30-INCH HEIGHT OF BURST 27-INCH
15-DEGREE V-BOTTOM VALLEY BURST ON AXIS

+ Top of Slope   ◊ Middle of Slope
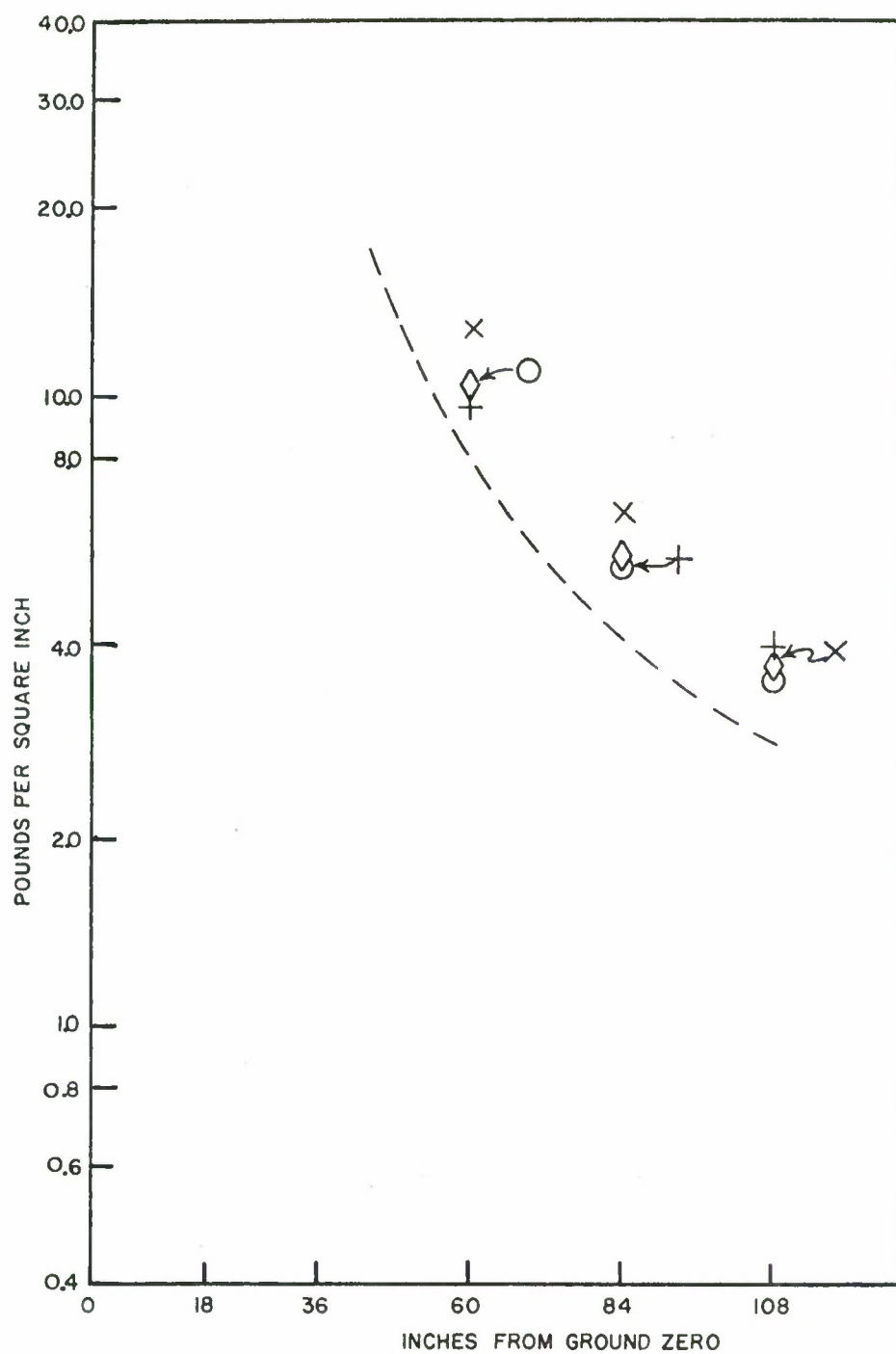O Bottom of Slope   ✕ Near the Bottom of Slope

Figure 32

PEAK PRESSURE DATA FOR 7-INCH HEIGHT OF BURST 27-INCH
V-BOTTOM VALLEY ON AXIS

+ Top of Slope   ◊ Middle of Slope
O Bottom of Slope   X Near the Bottom of Slope